DRL No. 214
DRD SE-6

DOE/JPL/956797--04
Distribution Category UC-63

DOE/JPL/956797--04

DE86 015247

FR-10092
August 1985

EXCIMER LASER ANNEALING TO FABRICATE LOW COST SOLAR CELLS

Final Technical Report

Contract No. 956797

Jet Propulsion Laboratory
Flat-Plate Solar Array Project
Module Performance and Failure Analysis Area

Prepared by: Anton Greenwald
Anton C. Greenwald, Principal Investigator

Approved by: Mark B. Spitzer
Mark B. Spitzer, Program Manager

SPIRE CORPORATION
Patriots Park
Bedford, MA 01730

LIST OF ILLUSTRATIONS

Numbers		Page
1	Experimental Laser Annealing Station	2-1
2	Photograph of Laser Annealing Apparatus	2-2
3	Pulsed Excimer Laser Beam Intensity (Arbitrary Scale) vs. Horizontal Distance	2-4
4a	Burn Patern from Excimer Laser at Focusing Lens	2-5
4b	Burn Pattern from Excimer Laser at Sample Position	2-5
5	Scanning Pattern for Annealing A 100cm^2 Sq. Wafer or 10 cm Diameter Round Wafer	2-6
6	Melting of Texture-Etched Surfaces	3-4
7	Light Reflection and Refraction on Texture Surface	3-5
8	Maximum Laser Line Width at Sample as a Function of Lens Position	3-8
9	Junction Depth vs Fluence for Laser Anneal	3-9
10	Damage to Polished Silicon Surface from PELA Due to Hot Spots	3-10
11	Screen Printed Front Contact Patterns on 100 mm Wafers and Polycrystalline Squares	3-15
12	Belt Furnace Temperature Profile	3-16
13	Evaporated Contact Pattern on 53 cm^2 Cell	4-8
14	Quantum Efficiency	4-15
15	Spreading Resistance Profiles	4-16

LIST OF TABLES

Numbers		Page
1	Process Sequence..	1-2
2	Effects of Texture Etching and Varying Fluence	3-3
3	Effect of Laser Wavelength	3-12
4	Effect of Post PELA Heating	3-13
5	Variables Used to Define Pattern for Screen Printed Contacts	3-15
6	Averaged Performance of Laser Annealed Cells with Screen Printed Contacts	3-18
7	Demonstration Experiment: Screen Printed Contacts on Laser Annealed Polycrystalline Material	3-19
8	Demonstration Experiment: Screen Printed Contacts on Laser Annealed Wafers	4-4
9	Demonstration Experiment: Evaporated Contacts on Laser Annealed Cells	4-9
10	Summary of Results for Demonstration Experiment	4-13
11	Process Definition for IPEG Analysis	5-2
12	Comparison of Operating Costs for 50 Watt KrF and XeCl Lasers . .	5-3
13	Requirements for Each Process Step	5-5
14	IPEG Analysis Summary	5-11

ABSTRACT

The objective of this program is to show the feasibility of using excimer lasers for cost effective annealing of ion-implanted emitters in the fabrication of silicon solar cells. The maximum AM1 efficiency achieved by the pulsed excimer laser anneal (PELA) process for n^+pp^+ cells was 15.6% for a 2 cm x 2 cm cell with photolithographically-patterned contacts. The maximum AM1 efficiency achieved by this PELA process for 100 mm diameter cells with screen printed contacts was 12%. These results are comparable with both diffused junction cells, and cells fabricated by ion-implantation and conventional furnace annealing.

IPEG analyses were used to estimate the cost of laser annealing, furnace annealing with passivating oxide growth, and diffused junction formation on a 3 MW/yr production line. The cost of laser annealing was estimated to be 4.9¢/watt compared to 7.1¢ per watt for the furnace anneal with oxide growth. However, the latter process was more cost effective. This study shows that the projected efficiency for ion-implanted laser annealed silicon solar cells would be 14%, compared to 16.4% with an oxide passivated furnace annealed cell, or an estimated 13% plus for a diffused junction cell. The module costs for these three processes were estimated as $6.56/watt , $5.81/watt, and $6.20/watt respectively. For crystalline silicon solar cells, ion-implantation with furnace anneal and surface oxide passivation would be the preferred process at this production level.

SECTION I
INTRODUCTION

The objective of this research contract is to determine if pulsed excimer lasers can be used in a cost effective way to fabricate crystalline silicon solar cells.

Pulse excimer laser annealing was initially developed by R.T. Young, W. Wilson, J. Narayan and others working at Oak Ridge National Laboratories.[1] Laser annealing of ion-implantation had been demonstrated in 1975[2] as had the related process of pulsed electron beam annealing.[3] However, early laser annealing processes suffered from microscopic beam non-uniformities which reduced the final efficiency of solar cells fabricated in this way. These non-uniformities were caused by high-coherence interference effects such as speckle.[4] Pulsed excimer lasers have an extremely short coherence length compared to ruby or Nd:Yag lasers, and therefore do not show diffraction effects or speckle in the beam.

The uniformity of the excimer laser beam is much better than that of the solid state lasers, even when using a beam homogenizer. The Oak Ridge group demonstrated that a small cell (p^+nn^+) fabricated by pulsed excimer laser annealing using non-overlapping pulses (one large area beam spot) could have an efficiency of 16.4%.[5] This result, plus the development of a commercial excimer laser usable by an operator who is not a laser engineer, were the basis for the work to be reported.

Technical work on this contract was organized into five tasks. The first task comprised selection of a fabrication process. The second task involved performance of experiments to optimize parameters for the use of the laser in the chosen process. The third task was to demonstrate that the laser source chosen had the required throughput for the production level envisioned. The fourth task involved a demonstration of a quantity of product fabricated using the chosen process sequence. The fifth and final task was to analyze the economics of the chosen process, and to make a comparison to the baseline process listed in Table 1.

TABLE 1. PROCESS SEQUENCE

Baseline	Pulsed Excimer Laser
Texture Etch	Bright Etch
Rinse	Rinse
Dry	Dry
Diffuse Junction	Ion-Implant Front
Aluminum BSF	Laser Anneal
Clean	
Print Ag Back	Print Ag Back
Print Ag Front	Print Ag Front
Laser Cut	Fire

Test and Sort
Cell Lay up
Prepare Materials
Lay Up
Bond, Heat, and Vacuum to module Lay up
Trim Seal
FINAL TEST
Package Module

To meet the objectives of this research program Spire chose a laser-based junction formation process which can be directly substituted for a typical diffused junction process presently in wide spread use in the PV manufacturing industry. The proposed process sequence was selected with a view to use low-risk technology that will be commercially available. In this way, successful demonstration should lead to rapid transfer of the technology to manufacturing operations.

The selected process sequence is shown in Table I compared to a conventional process sequence. The new process replaces gaseous diffusion with ion-implantation and pulsed excimer laser annealing (PELA). Texture etching is replaced by isotropic etching in the initial wafer cleaning process because the laser cannot uniformly irradiate this surface (Section 3.1). The hydroflouric acid cleaning step needed after gaseous diffusion is deleted in the new laser-based process sequence because ion-implantation and laser annealing are inherently clean processes which do not grow oxides or glasses. Also, ion-implantation does not produce a shunting junction on the edge of the wafer, so coin-stack edge etching is deleted from the baseline process sequence. Gaseous diffusion requires aluminum deposition and firing to produce a back surface field (BSF) and to counterdope the backside junction in the diffusion process, but this step can be skipped for the PELA process sequence if the resistivity of the silicon is low enough to obviate a BSF. The deletion of three process steps: texture-etching, plasma edge etching, and HF clean, simplify the PELA processes sequence.

SECTION 2
APPARATUS

This section describes in detail the annealing apparatus used in this work. A schematic diagram of the experimental laser annealer is shown in Figure 1. A photograph of the apparatus with a two inch diameter sample partially annealed is shown in Figure 2. The sample and focusing optics were mounted on an optical table that was separate from the laser that was mounted on a cart. Positioning of the laser relative to the optical table was not critical, and was adjusted to ± 1/8 inch at best. As shown in Figure 1, a small optical bench was mounted vertically on the optical table to hold a 45° mirror with an AR coating that reflected the laser beam from the horizontal to the vertical. A cylindrical focusing lens, also mounted on the vertical rail, was chosen to image the rectangular beam from the laser (about 1 cm x 2 cm) onto the wafer surface (nominal spot size 0.7 mm x 30 mm). The lens was plano-convex with the flat side up.

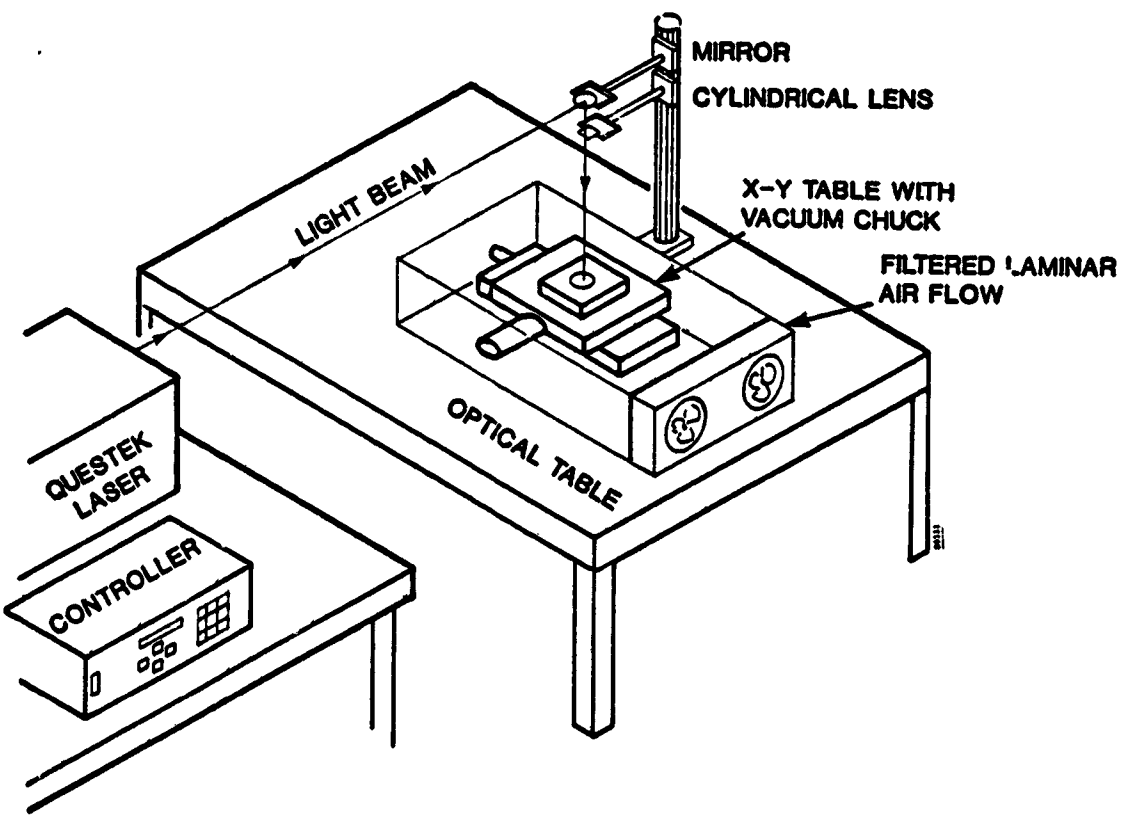

FIGURE 1. EXPERIMENTAL LASER ANNEALING STATION.

The sample was held on a vacuum chuck mounted on an x-y translation stage. The flatness and accuracy of positioning this stage were within 0.05mm . The alignment of the lens and its distance to the sample holder were set by vernier to within ± 0.1 mm. A micrometer adjustment for controlling the focus was available but was not needed. As shown in Figure 2, the sample translation stage, but not the focusing lens, was placed inside of a clean air hood. A hole was cut out for light transmission through the plastic hood near the lens. Because this plastic absorbed ultra-violet light it acted as a safety shield against stray reflected light. A small dedicated computer controller moved the stage and triggered laser firing.

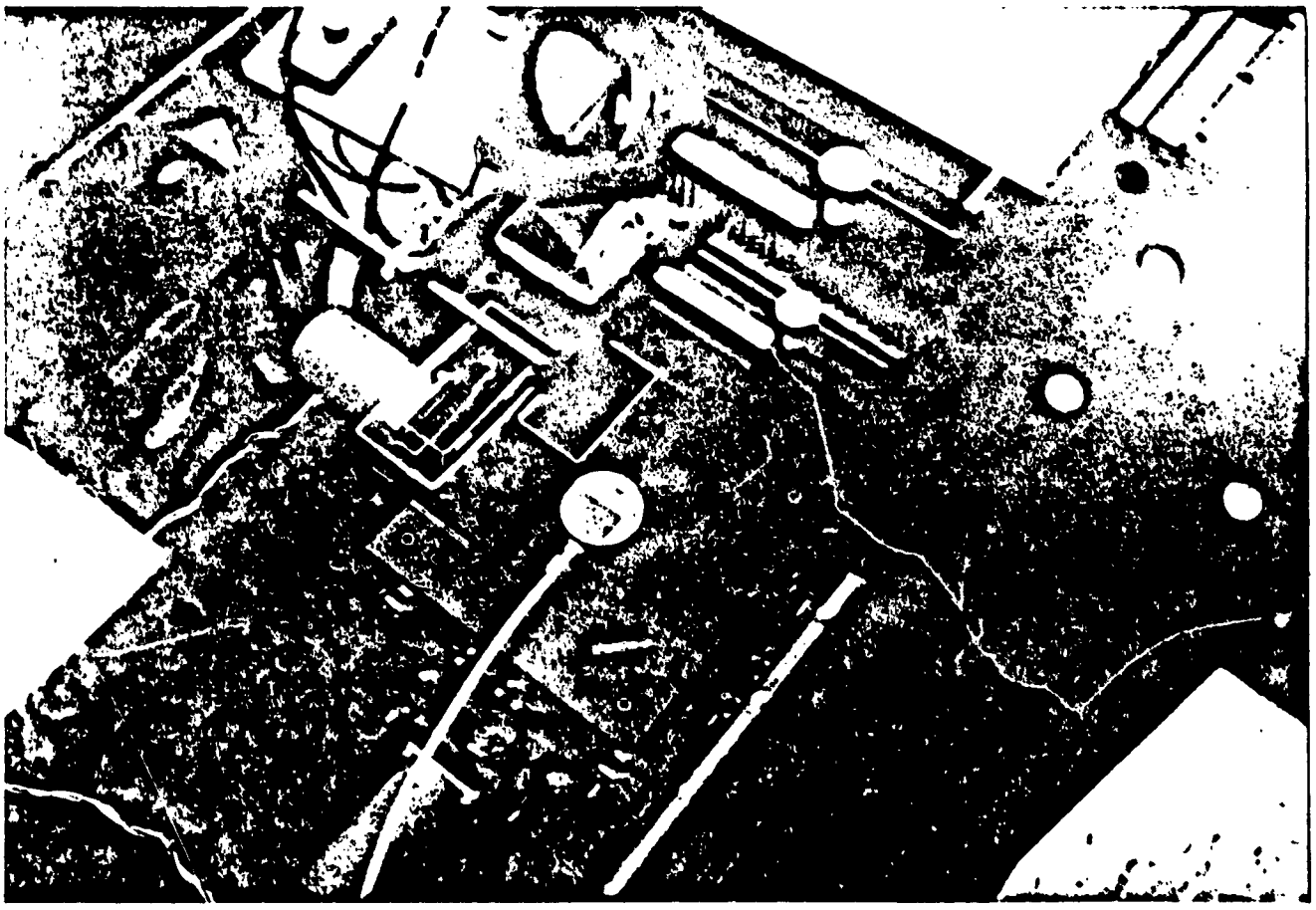

FIGURE 2. PHOTOGRAPH OF LASER ANNEALING APPARATUS.
(Darker part of sample shown has been annealed.)

The laser used was a Questek model 2200[6] (see Appendix A). Actually, five different lasers were used in the course of this study. Each was made available during the manufacturer's final testing. The results did not vary with different instruments of the same model. Figure 3 illustrates the output of the laser at its lens.

The uniformity of the laser beam at the output of the laser (when properly adjusted) is shown in Figure 3. The intensity profile was measured along a line bisecting the horizontal beam. It is uniform within 2% over the flat portion of the top hat shape. Non-uniformities in this beam profile could be detected by a non-uniform annealing pattern on silicon or by using thermal sensitive paper (Figure 4). Maintaining the uniformity of this beam in production was not judged to be a problem.

The pattern of the beam at the sample position is shown in Figure 4. The width of the beam was measured at its greatest part in the most uniformly burned region of the thermal paper. The length of the beam was measured between end points taken at the half-width of the beam. The fluence was calculated as total energy divided by beam area (length times width). To anneal a large area, the beam spot, nominally 0.7 mm by 30 mm, had to be overlapped. The typical scanning pattern is shown in Figure 5. Movement of the sample in both a continuous and stepwise fashion was tested. No distinction in results could be discerned for pulsing the wafer while in continuous motion (up to 10 cm/sec) or when stopped for step and repeat pulsing in which the laser was triggered at each position.

The output power of the beam was monitored on every pulse by using a beam splitter and detector internal to the laser. The pulse energy was displayed on the laser console and held constant by a microprocessor which could adjust the power supply voltage. When the voltage across the discharge electrodes reaches its maximum value the microprocessor can no longer maintain a constant light output and an alarm is sounded to indicate that a change of gas is needed. Under microprocessor control the stability of the pulse-to-pulse output energy was better than $\pm$ 5%.

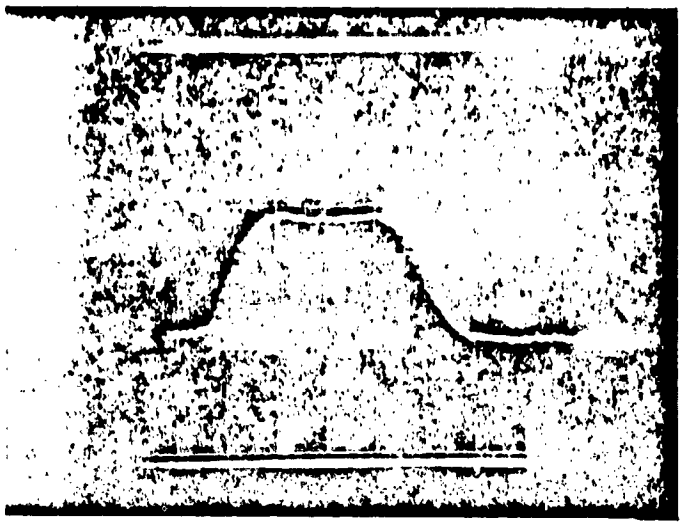

FIGURE 3. PULSED EXCIMER LASER BEAM INTENSITY (ARBITRARY SCALE) VERSUS HORIZONTAL DISTANCE (5 mm per division) AT OUTPUT LENS.

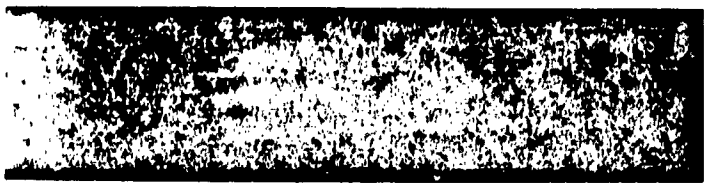

FIGURE 4a. BURN PATTERN FROM EXCIMER LASER AT FOCUSING LENS (APPROXIMATE FLUENCE 0.1 J/cm^2 AT 308 nm).

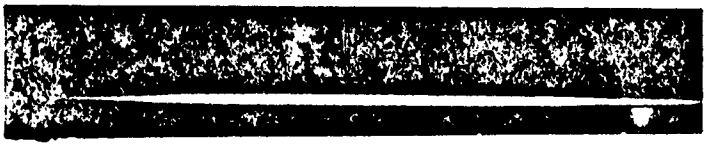

FIGURE 4b. BURN PATTERN FROM EXCIMER LASER AT SAMPLE POSITION (Same pulse as above, approximate fluence 1.0 J/cm^2).

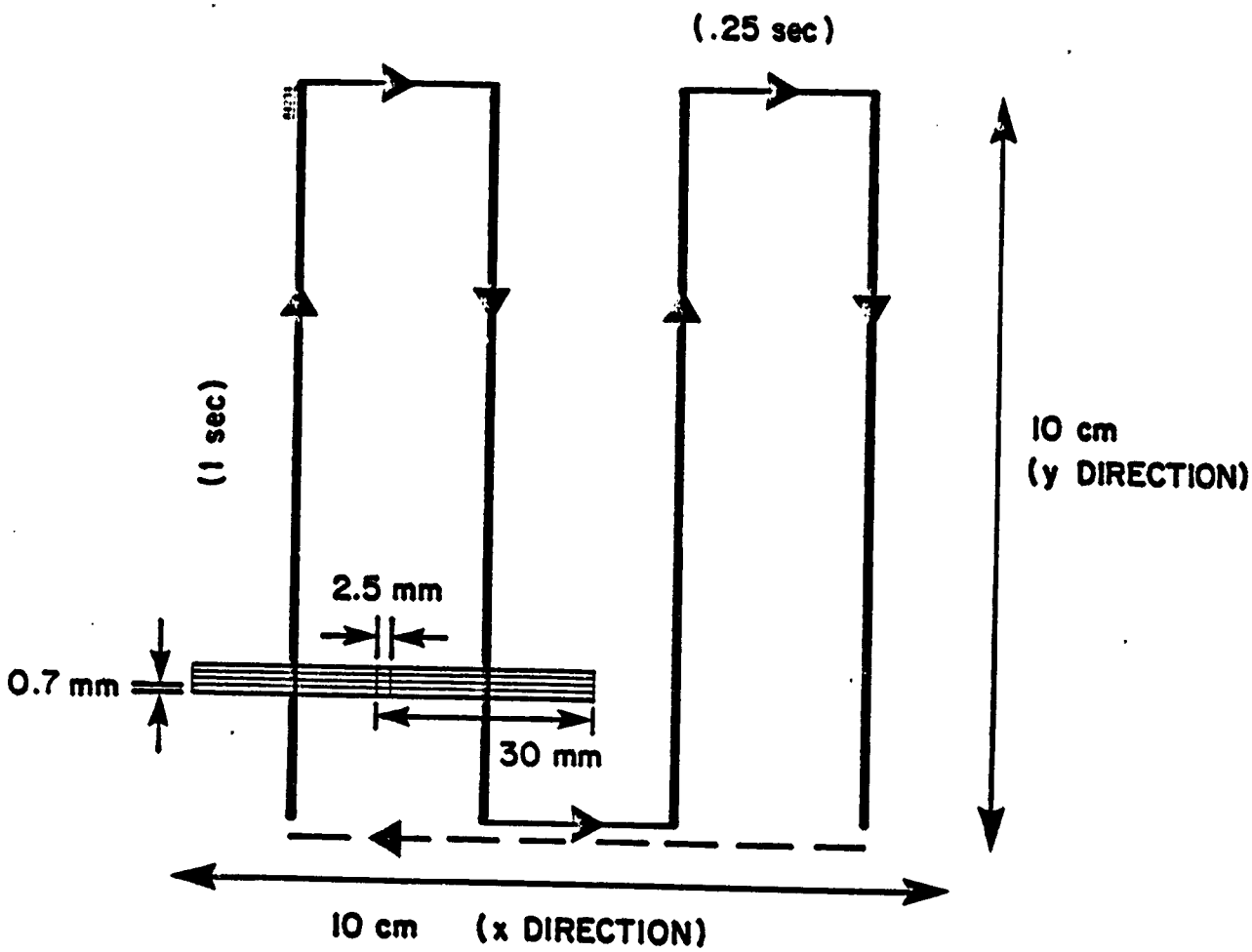

FIGURE 5. SCANNING PATTERN FOR ANNEALING A 100 cm^2 SQUARE WAFER OR 10 cm DIAMETER ROUND WAFER (Total transit time at 10 cm/sec is 5.5 seconds.)

The front surface reflecting mirror was silvered and AR coated for 45° angle of incidence at 275 nm (halfway between KrF and XeCl wavelengths). The initial cylindrical focussing lens was plano-convex with both sides coated like the mirror. Self-focusing effects in the beam damaged tne AR coating although the energy density (neglecting self-focusing effects) was only 0.1 J/cm^2 or lower at this optical component. An uncoated cylindrical lens reduced the transparency at 248 nm to 80% compared to 82% for the coated lens. Both lenses were fabricated from the purest quality synthetic quartz (Suprasil II or equivalent).

SECTION 3
PROCESS DEVELOPMENT

The following parameters are known to influence the results of laser annealing of ion-implantation damage: surface preparation, type of ion implanted, ion-implant energy and dose, sample temperature and atmosphere during laser anneal, the uniformity and fluence of the laser beam, pulse width (or scan rate and spot size when using cw lasers), wavelength, percent overlap of beam on successive pulses, and post-pulse thermal annealing.

The parameter space described above was too large to investigate completely in a one year program. Based upon past experiments at Spire Corporation with pulsed electron beam annealing[7] the following ion-implantation parameters were fixed: phosphorus implants at 10 keV to a dose of 2.5×10^{15} ions/cm^2, normal to the sample surface. Implants were carried out on the SPI-ION™ 1000 non-mass analyzed ion-implanter.

Several laser parameters were fixed. Young et al. reported that a shorter pulse width resulted in a deeper junction for fixed fluence, and lowered the threshold for annealing.[8] Based on this data and the design of the laser used, a pulse width of 25 ns was used in all experiments reported herein. Also, because Young et al. reported no advantage to heating the wafer during pulsed excimer laser annealing,[1] all experiments performed in this program maintained the samples at room temperature during pulse processing. All samples were annealed in a filtered air stream to minimize dust effects. Laser annealing in air grows a thin oxide layer on the wafer surface, but this layer is not passivating and does not affect device performance. Also, this oxide layer is too thin to interfere with contact metallization by screen printing.

All silicon material used for this program, with one exception, was boron doped typically 1 to 2 ohm-cm and (100) orientation. Both float zone and Czochralski (CZ) material were used. Two and three inch diameter wafers were used to determine the effect of varying laser parameters while 100 mm diameter material was used to develop screen printing processes compatible with annealing.

The typical process sequence used in experiments is described below. All wafers were cleaned after scribing identification numbers on their backs. They were then implanted and cleaned again. Wafers were stored in a dry nitrogen box prior to laser annealing. After laser annealing the wafers were cleaned a third time and selected controls were heated in a furnace. For screen printed contacts, the backs were inked, dried and fired. Ink was then applied to the front, dried and fired. Some cells were then dipped in buffered HF. For evaporation contacts, photoresist was applied to the wafer front surface, prebaked, exposed, developed, and the front contact (Ti-Pd-Ag) was evaporated immediately after an HF dip to remove the native oxide layer. This was followed by lift-off, cleaning, evaporation of the back contact at 200°C (Al-Ti-Pd-Ag) and sintering at 400°C for five minutes. The evaporated contacts were plated to a thickness of 8 to 10 micrometers, and then cells were sawed out of the wafers; either six 2x2 cm or one 53 cm^2 cell per 100 mm wafer. Evaporated AR coatings (Ta_2O_5) were applied to some wafers. Variations on this process sequence, such as thermal heating after laser annealing, are described later.

The effects of the following parameters were studied in detail: surface preparation, fluence, laser wavelength, and post-PELA thermal history.

3.1 EFFECT OF TEXTURE-ETCHING

Previous reports[9] implied that laser annealing of texture-etched silicon surfaces was feasible. However, good results were not achieved when irradiating this surface structure with an excimer laser. Experimental results are summarized in Table 2. At low fluence it appears that the surface is unannealed, while at high fluence it appears that the surface is damaged. Figure 6 shows photomicrographs of the melted surface.

The effects seen may be explained by the light ray diagram of Figure 7. Incident light must make at least two reflections off this surface relief before any light is reflected. The illumination of all of the surface is uniform for a uniform source on the first incident (reflected) beam, but it is not uniform for the second reflection. In particular, the base of the pyramids receives about twice the fluence seen at the top. Thus one part of the surface must be unannealed, or the other part over-melted. Note that this laser melts a very thin (~100Å) layer of the silicon very quickly and that

TABLE 2. EFFECTS OF TEXTURE ETCHING AND VARYING FLUENCE

CELL ID	V_{oc} (mV)	J_{sc} (mA/cm^2	F.F. %	(No AR) Eff. %	With AR) Eff. %	Laser fluence (J/cm^2
Polished Surface						
39-20a	481	16.2	66.3	5.2	7.3	0.5
20-11b	532	22.4	61.4	7.3	10.2	0.8
20-6a	545	23.0	65.4	8.2	11.5	1.0
20-7a	534	22.9	61.8	7.6	10.6	1.1
20-10b	560	23.4	74.2	9.7	13.6	1.2
20-9b	578	23.0	78.6	10.5	14.7	1.8
39-23a	586	22.8	78.9	10.5	14.7	furnace control
Textured Surface						
40-18b	476	27.4	68.5	8.9	-	0.5
19-9b	522	27.6	60.7	8.7	-	0.8
19-12a	552	28.2	75.5	11.8	-	1.0
19-6a	552	26.0	75.1	10.8	12.6	1.1
19-7a	537	26.0	75.3	10.5	12.3	1.2
19-4a	568	22.6	63.5	8.2	10.7	1.8
19-8a	583	29.5	75.3	12.9	15.1	furnace control

* x 1.4 eff. with no AR for polished surface.

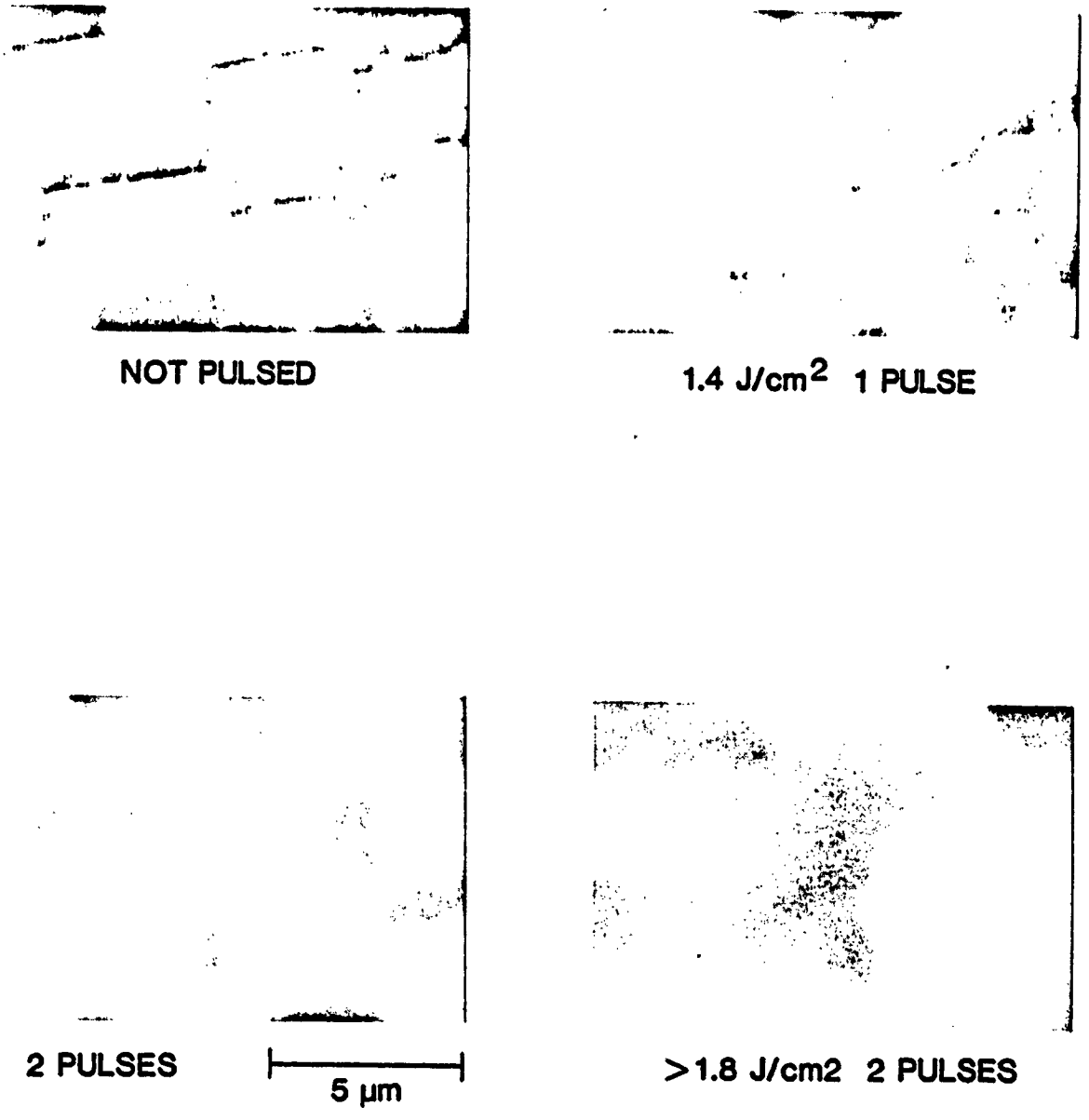

FIGURE 6. MELTING OF TEXTURE-ETCHED SURFACES.

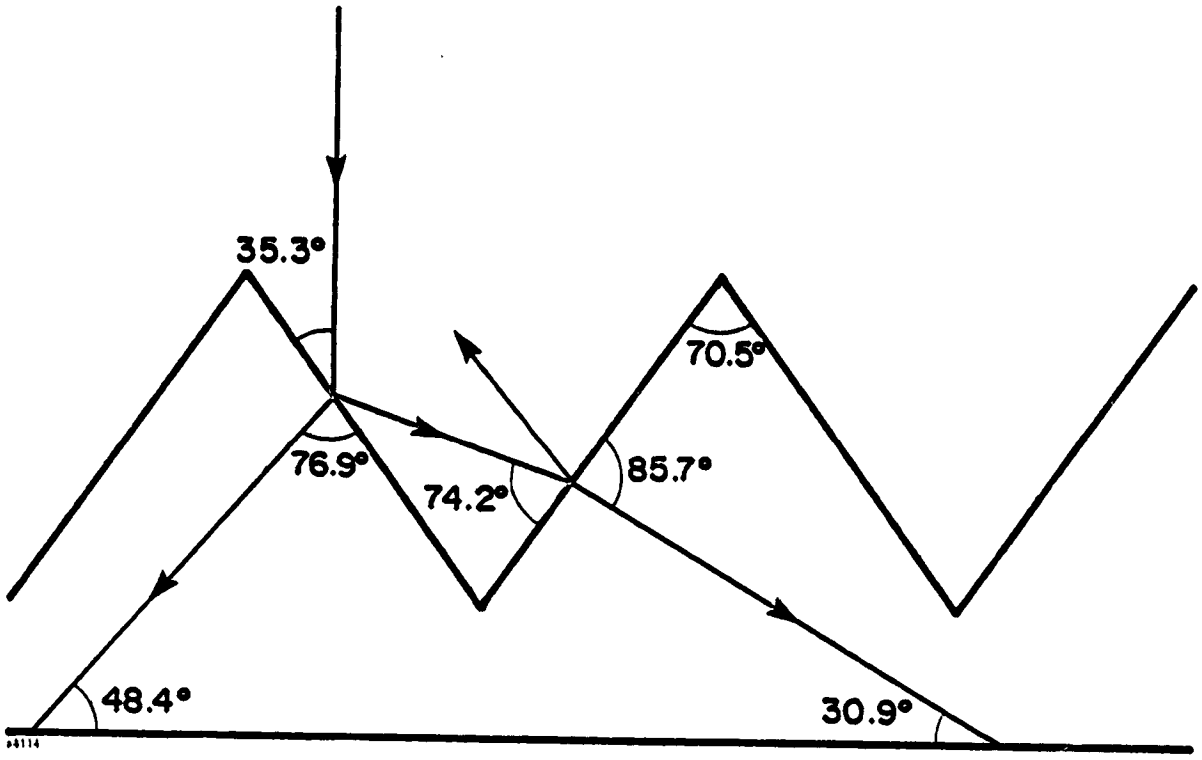

FIGURE 7. LIGHT REFLECTION AND REFRACTION ON TEXTURED SURFACE.

the coefficient for reflection from this molten surface is 0.6,[10] so that the power density incident on the second reflection is nearly equal to that in the primary laser beam.

Some solar cells were fabricated by applying evaporated contacts to excimer laser annealed texture-etched surfaces (Table 2). The maximum output power from any of these cells was about 90% that of the furnace annealed control, while the maximum output power from laser annealed polished surfaces was comparable to the furnace annealed control. All attempts to form screen-printed contacts to this textured material resulted in badly shunted junctions. Therefore, all work for the demonstration experiment was performed on polished or bright-etched surfaces.

3.2 EFFECT OF FLUENCE

The term fluence is used to described the time-integrated power density of the laser beam at the sample surface over the full pulse width. For the short pulsed laser used, the nature of the intensity-time profile will not significantly alter the results, provided that the pulse width is constant.

The fluence of the laser beam at the sample position could not be measured directly because the energy density typically utilized would damage power meters. The fluence was calculated from the total energy measured in one pulse at the laser and the irradiated spot size burned in thermally sensitive paper (Figure 4). The Questek excimer laser has an internal power meter which measured the energy of each pulse using a beam splitter. Ths internal meter was calibrated by comparing readings to an external power meter, traceable to NBS standards, placed at the beam exit of the laser. In addition, this external power meter was used to measure the intensity of the beam about one inch below the focusing lens. About 82% of the laser output power reached the power meter below the lens at a wavelength of 308 nm; 80% of the total output reached the power meter at 248 nm. Slits were placed on top of the focussing lens to determine the power lost to stray light not in the most intense part of beam. Stray light accounted for less than 1% of the total beam power.

The fluence of the beam could be changed with high relative accuracy by varying the energy output of the laser. The energy per pulse could be varied at either wavelength

within the range of 300 to 500 millijoules. The energy used most often was 400 mJ per pulse. The fluence could also be varied by changing the position of the focusing lens to vary the beam width, as shown in Figure 8. The length of the beam spot was altered very little when the position of the lens was changed.

There are two physically important effects of varying the fluence for pulsed excimer laser annealing. First, there is a threshold value which is the minimum fluence required to melt a very thin layer of the silicon surface. This minimum will vary with wavelength, surface preparation and implant parameters. From experiments performed in this program, the minimum value for polished wafers with shallow, high dose phosphorus implants was about 1.0 J/cm^2. The second physical effect is that increasing the fluence increases the depth of melt. Since the dopant diffuses rapidly in the molten silicon, increasing the fluence will increase the junction depth (Figure 9). For a fluence near the threshold value, increasing the junction depth is beneficial because ion-implant damage extends well below the depth of the peak dose. This damage is not removed unless the melt depth during laser anneal is greater than the depth of the damaged region, or unless there are other high temperature thermal processing steps which will anneal the damage. Electrically this damage contributes to excess leakage current which degrades solar cell performance. Removal of residual damage with increasing junction (or melt) depth is believed to be the cause of increasing cell efficiency with increasing fluence seen in Table 2.

At high fluence levels the surface of the silicon may be damaged (Figure 10). Because scattered light was seen from the sample surface when this type of damage appeared, it is believed that a small amount of silicon in a very thin layer near the surface was vaporized. The observed light was emitted by the vapor as a result of chemical reactions or fluorescence. The shock wave produced by this vaporization spalled some further molten material into the crater-like pattern seen in Figure 10. As long as the continuity of the emitter region was not interrupted by the damage, the resulting solar cell was still functional. Metallization over the damaged region did not shunt the junction. A loss in power generated approximately proportional to the total damaged area of the cell was measured.

At high fluence levels between the damage threshold (fluence unknown) and the maximum tested with a uniform beam, about 2 J/cm^2, power will be lost in the resulting

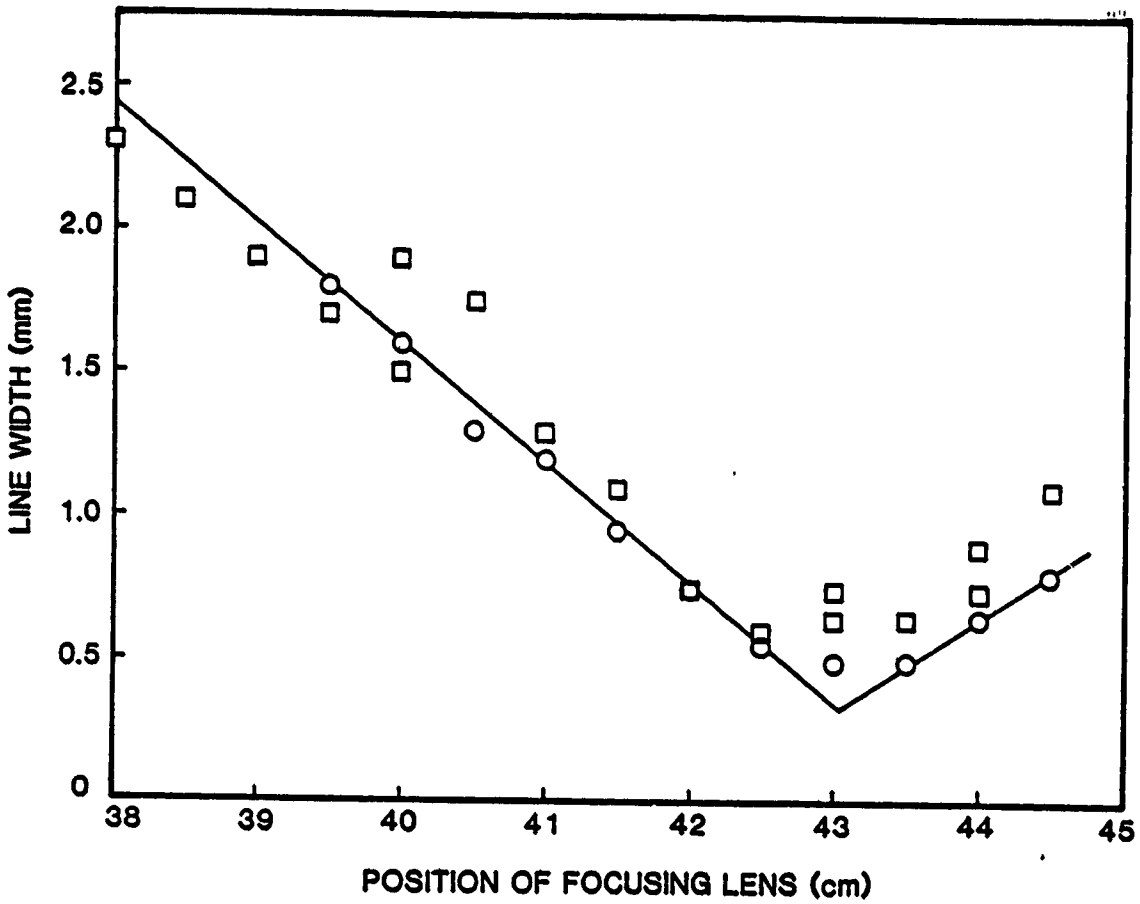

FIGURE 8. MAXIMUM LASER LINE WIDTH AT SAMPLE AS A FUNCTION OF LENS POSITION.

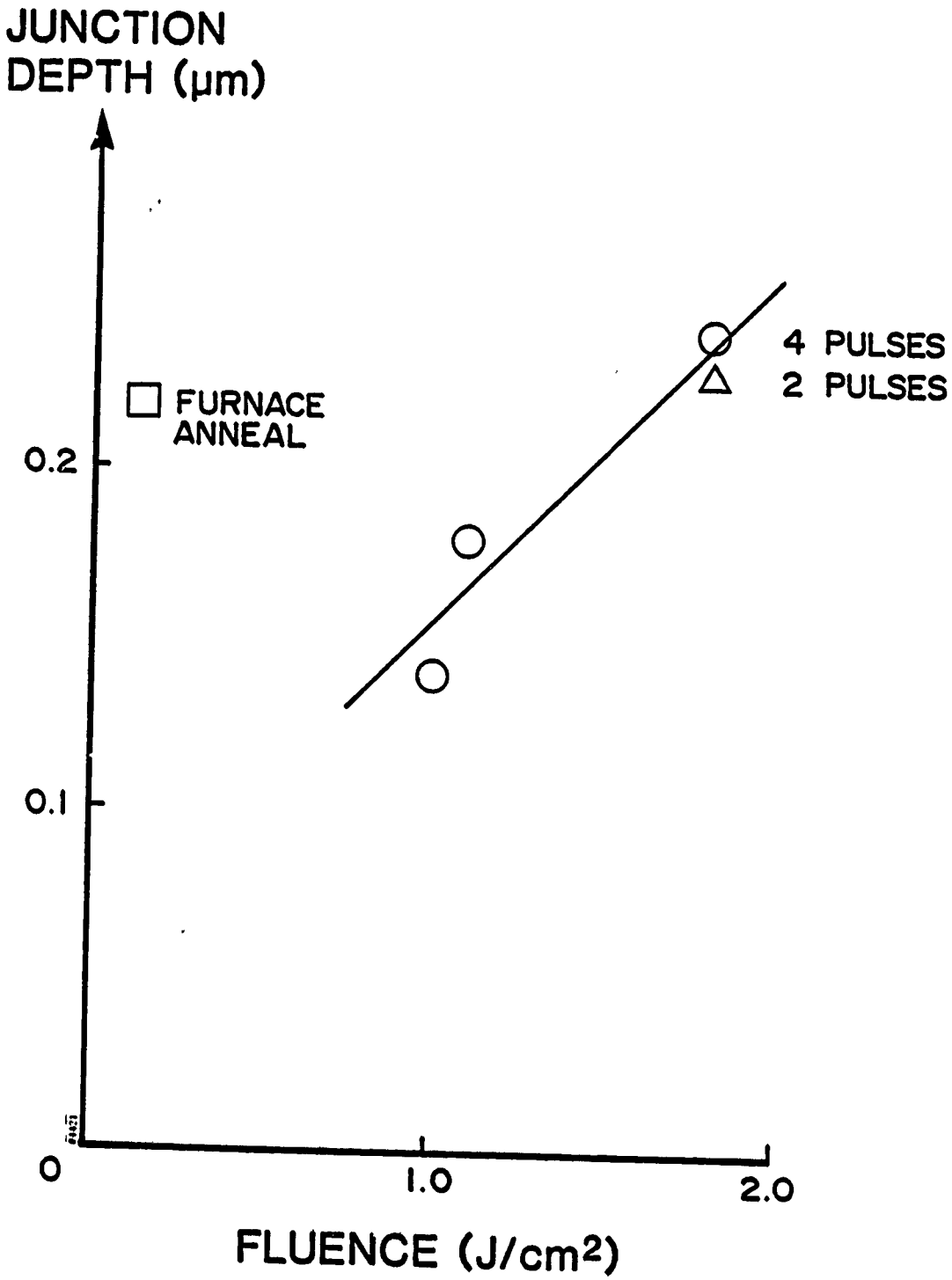

FIGURE 9. JUNCTION DEPTH VERSUS FLUENCE FOR LASER ANNEAL.

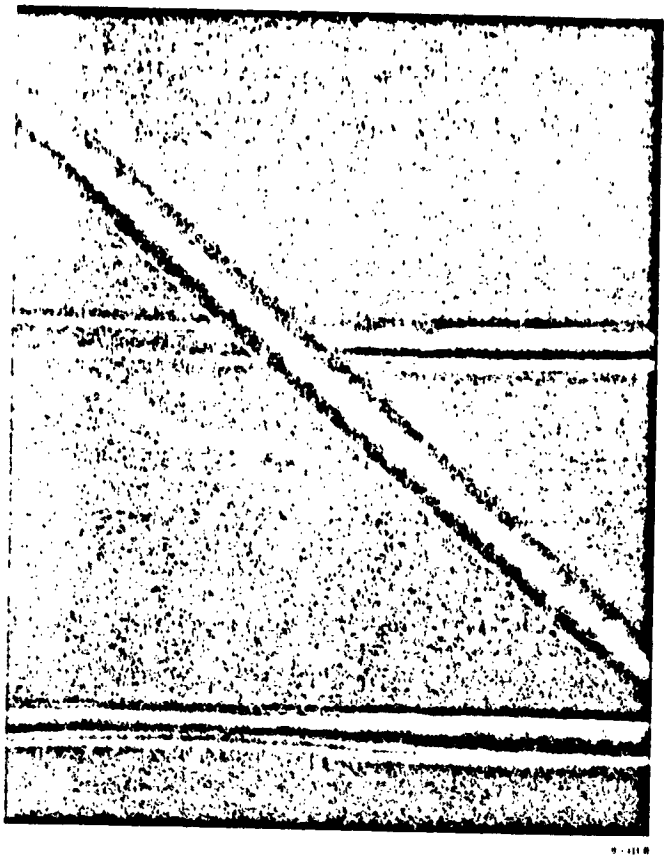

FIGURE 10. DAMAGE TO POLISHED SILICON SURFACE FROM PELA DUE TO HOT SPOTS. (Damage areas are horizontal features, solar cell metallization is diagonal line, magnification 200x).

laser annealed cell due to a excessively thick emitter layer that absorbs short wavelength light in a region with a very low minority carrier lifetime. High fluence levels were not tested in this program.

3.3 EFFECT OF WAVELENGTH

Pulsed excimer laser annealing experiments were performed using two types of gas fills, Kr and F_2 or Xe and HCl. The two corresponding wavelengths are 248 nm and 308 nm. The light output of an excimer laser using KrF is typically 50% higher than the light output of any other gas fill at any other wavelength, assuming equal input power. Also the number of pulses which can be obtained from a typical single fill of Kr, F_2, plus buffer gas is greater than the number of pulses for any other gas mixture except XeCl. The light output for Xe, HCl, plus buffer gas is greater than the output for any other gas mixture except KrF, and the number of pulses which can be obtained from a single fill for this gas mixture is greater than for any other. The economic comparison is treated in detail in Section 5. For potential production use in annealing there is no reason to use shorter or longer wavelengths and the choice in this work was limited to KrF and XeCl.

Experiments in annealing float-zone silicon wafers and fabrication of solar cells using either 248 nm or 308 nm light are summarized in Table 3. No statistically significant variation could be seen in cell efficiency. There is no technical reason to prefer 248 or 308 nm light, only economical incentives apply. (Note that ozone generation is minimal with either source and other safety issues are comparable).

3.4 EFFECT OF POST PELA THERMAL TREATMENT

Several authors[11, 12] have suggested that heating the wafers during or after pulsed laser annealing would improve results. The improvement was more noticeable when using pulsed Nd:Yag lasers, with conflicting results for pulsed excimer lasers.[1] Three different experiments were performed in this program to test the effect of post PELA thermal processing of the wafers. Typical time-temperature cycles were 650°C for 5 minutes in nitrogen, a cycle which could alloy an aluminum back contact. The results, presented in Table 4 are mixed. Some cells were improved by the thermal treatment, some cells were degraded. We believe that some form of contamination reduced the minority carrier lifetime in those cells that were degraded by the thermal cycle.

TABLE 3. EFFECT OF LASER WAVELENGTH

ID	Fluence J/cm^2	λ (nm)	R series ohms	MCDL μm	J_o pA/cm^2	V_{oc} mV	J_{sc} mA/cm^2	FF %	EFF. %
4539									
13a		Furnace Anneal	--	--	--	590	23.4	78.0	10.8
13b		Furnace Anneal	.349	155	3.2	591	23.3	78.7	10.9
14a	1.3	248	.333	79	67.1	508	22.5	75.4	8.6
14b	1.3	248	--	--	--	509	22.5	73.6	8.4
15a	1.5	248	--	--	--	568	21.3	75.8	9.1
15b	1.5	248	.319	59	6.4	568	21.3	76.8	9.3
16a	2.0	248	--	--	--	565	20.3	72.5	8.3
16b	2.0	248	.256	31	6.6	565	20.2	74.5	8.5
17a	1.0	248	--	--	--	494	20.9	74.7	7.7
17b	1.0	248	.478	56	112.	494	20.8	75.7	7.8
18a	1.3	308	.318	60	9.3	554	21.2	71.1	8.4
18b	1.3	308	--	--	--	553	21.2	68.9	8.1
19a	1.5	308	2.9	14	7.0	549	19.6	48.4	5.2
19b	1.5	308	--	10	9.2	489	20.7	32.6	3.3
20a	1.5	308	.329	58	6.4	560	20.6	61.0	7.0
20b	1.5	308	--	--	--	555	20.7	56.1	6.4
21a	2.0	308	.264	62	6.1	562	20.4	52.5	7.2
21b	2.0	308	--	--	--	549	20.1	49.5	5.5
22a	1.0	308	--	--	--	528	21.2	73.3	8.2
22b	1.0	308	.341	52	24.6	531	21.2	75.6	8.5
4540									
2a	1.3	248	--	--	--	506	27.6	66.9	9.4
2b	1.3	248	.378	129	54.6	514	28.1	72.5	10.5
3a	.8	248	--	--	--	483	27.7	71.0	9.5
3b	.8	248	.435	89	158.	488	27.8	72.4	9.8
22a	1.0	308	--	--	--	527	27.7	60.5	8.8
22b	1.0	308	.463	128	42.7	522	27.1	68.4	9.7
23a	1.3	308	--	--	--	499	24.6	44.1	5.4
24a	1.0	308	.294	134	25.2	509	27.1	47.8	6.6
25a	.8	308	--	--	--	512	28.9	61.2	9.0
25b	.8	308	.334	137	54.9	509	28.1	64.1	9.1

Note: No AR coatings employed. Cell area is 4 cm^2.

TABLE 4. EFFECT OF POST-PELA HEATING

ID	Fluence J/cm^2	λ (nm)	Overlap %	# passes	Post PELA temp	R series ohms	MCDL μm	J_o pA/cm^2	V_{oc} mV	J_{sc} mA/cm^2	FF. %	EFF. %
4539												
5a	Furnace Anneal					.250	149	3.7	584	23.3	75.7	10.3
5b	Furnace Anneal					.290	145	4.0	577	23.1	64.3	8.6
6a	1.5	308	60	1	--	.330	43	6.2	565	20.4	73.0	8.4
6b	1.5	308	60	1	--	--	--	--	557	20.4	59.2	6.7
7a	1.5	308	60	1	650	--	--	--	575	21.9	60.8	7.7
7b	1.5	308	60	1	650	.176	97	4.3	577	21.8	75.0	9.4
8a	1.5	308	60	1	--	.269	41	6.7	565	20.2	76.8	8.7
8b	1.5	308	60	1	--	--	--	--	561	20.2	72.6	8.2
9a	1.8	308	50	1	650	--	--	--	570	20.3	75.0	8.7
9b	1.8	308	50	1	650	.205	56	5.6	571	20.4	75.8	8.8
10a	.9	308	85	1	--	1.980	46	42.9	516	21.5	72.8	8.1
10b	.9	308	85	1	--	--	--	--	510	21.1	70.1	7.5
11a	.9	308	85	2	650	.378	65	6.9	568	22.2	73.9	9.3
11b	.9	308	85	2	650	.407	70	7.1	564	22.3	69.8	8.8
12a	1.5/.9	308	60/85	2	--	.276	74	6.1	568	21.1	72.7	8.7
12b	1.5/.9	308	60/85	2	--	--	--	--	564	21.4	64.4	7.8
4540												
1a	1.1	308	80	1	650	--	--	--	525	26.1	57.6	7.9
1b	1.1	308	80	1	650	.258	87	18.8	539	27.0	64.5	9.4
7a	1.1	308	80	1	650	--	--	--	512	25.6	50.1	6.6
7b	1.1	308	80	1	650	--	--	--	523	26.2	42.9	5.9
8a	Furnace Anneal					--	--	--	553	29.0	61.1	9.8
8b	Furnace Anneal					.301	192	11.1	567	28.4	21.2	11.5
10a	1.1	308	80	1	--	.255	132	32.4	523	28.1	62.5	9.2
10b	1.1	308	80	1	--	--	--	--	521	27.8	63.3	9.2
12b	1.1	308	80	1	--	--	--	--	508	28.1	46.0	6.6
15a	1.1	308	80	1	--	--	--	--	509	27.4	57.3	8.0

Note: No AR coatings employed. Area is 4 cm^2.

In some of the wafers the post-PELA thermal cycle had no effect (presumably not contaminated). The comparison between screen printed contacts fired at over 750°C and evaporated contacts sintered below 400°C in Section 4 supports this result. Heating of ion-implanted wafers during or following PELA does not appear to be advantageous.

3.5 SCREEN PRINTED CONTACTS

The development of low cost contacts for ion-implanted and excimer laser annealed cells was based on the thick film technology. This technology is widely utilized in the production lines of most manufactures of silicon solar cells today, and represents an accepted mass-production technique. The experimental development took the following path: screen design and fabrication, furnace profile adjustments, ink analysis, and a mock production run.

The grid pattern optimization utilized a computer analysis of contact loss mechanisms to design the grid spacing. Two designs were generated, the first for printed line widths of 7 mils and the second for 15 mil widths Table 5 indicates the other variables used in the optimization program.

The optimal value for grid spacing was determined to be 120 mils for the narrow line widths and 280 mils for the wide line widths. A sample analysis of loss for the 7 mil width gave a power loss due to contacts of 12% with 6% due to shadowing, 3% due to sheet resistance and 3% due to bulk metal resistance. No provision for contact resistance, a potentially major component in thick film contacts, was available in the model. The front grid pattern was then fabricated on a stainless steel screen. An emulsion thickness of 0.5 mils gave the best results, with a surprising sensitivity of cell results to this variable. Figure 11 shows the front pattern. Note that the SPIRE logo is deleted on functional cells. The back metal print was a full-area contact.

Development of an acceptable firing profile was a very important issue in light of past reported difficulties with thick film contacts on ion-implanted wafers. We used an infrared belt furnace to achieve fast firing. Although we made several modifications to the furnace in an attempt to achieve the required spike profile, we were never able to achieve the necessary fast cool-down required for the ink we used. A recorder tracing

TABLE 5. VARIABLES USED TO DEFINE PATTERN FOR SCREEN PRINTED CONTACTS

Wafer Sheet Resistivity	50	ohms/square
Voltage at Maximum Power	0.45	volts
Current Density at Maximum Power	0.03	amps/cm^2
Metal Bulk Resistivity	12	micro-ohm-cm
Contact Height	15	micrometers

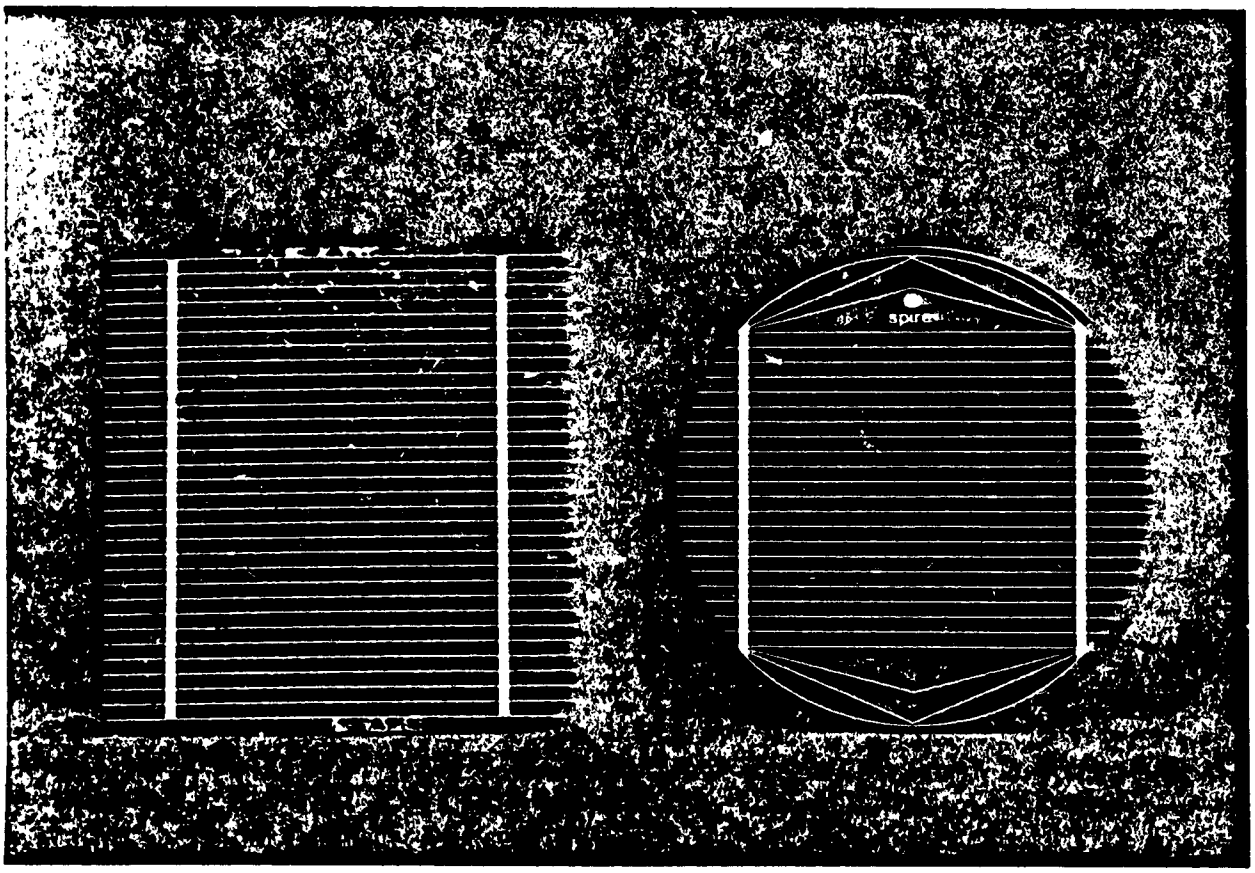

FIGURE 11. SCREEN PRINTED FRONT CONTACT PATTERNS ON 100 mm WAFERS AND POLYCRYSTALLINE SQUARES.

of the profile of the furnace temperature is shown in Figure 12 as determined by a thermocouple mounted between two ceramic plates. There is some question as to whether this is indicative of the profile a silicon wafer would experience, but it was a means of establishing a best case and reproducing it. Over the course of the process development many different profiles were attempted, but this particular profile gave the most consistent cell characteristics.

Constrained by both the number of wafers to process and the time in which to develop that process, we decided to limit our analysis to only a few inks from one manufacturer. Previous experience with Thick Film Systems (TFS) ink had been favorable, so those products were chosen. Initial experiments were performed on ion-implanted wafers which were furnace annealed, as these were more readily available.

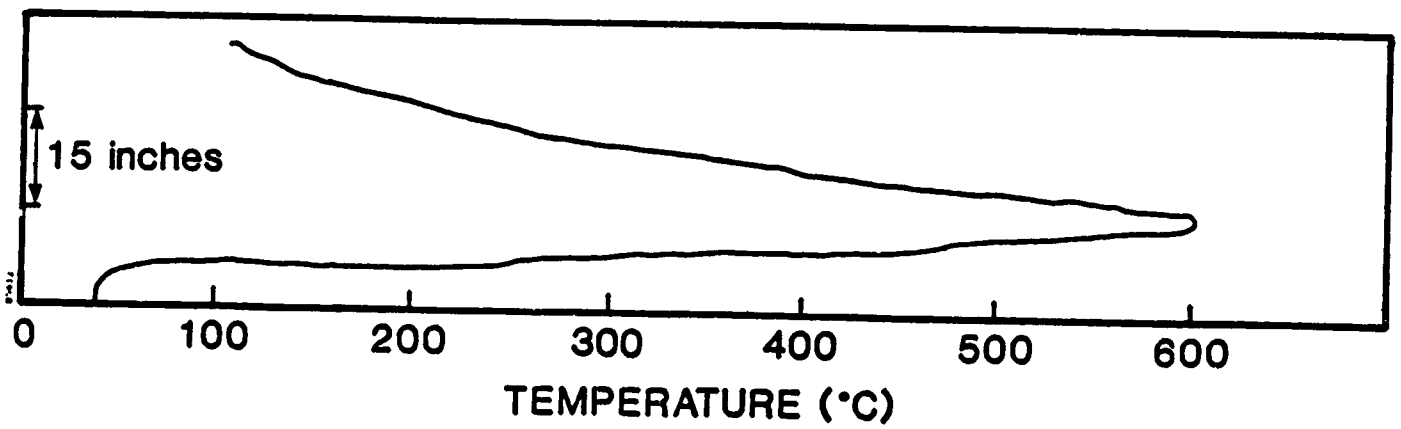

FIGURE 12. BELT FURNACE TEMPERATURE PROFILE (RECORDER TRACING).

After discussion with TFS* we decided to use a new low-temperature firing ink, #3350. We attempted to co-fire the fronts and backs, using either G505 or 3398: both Ag with 3% Al doping for the back contacts. The best results on cells were 9.5% to 10% on polished wafers. The same experiment on diffused wafers (same wafer manufacturer and lot) also gave the same results, thereby indicating that there are no inherent limitations in applying screen printing to the ion-implanted wafers. One recurring difficulty was the fill factor, we require a brief HF etch to achieve 70% fill factors. The front ink was the difficulty, and we found that it was low-temperature glass, but of higher content than the 5% normally required for good as-fired results.

We then went exclusively to the (proprietary) doped Ag front ink #3349 for the remainder of the development work. Using this ink, and a longer firing schedule on the back ink, we achieved a best result of 74% fill factor (as fired) on diffused wafers. We were unable to subsequently repeat those results on either diffused or ion-implanted, and had to resort to HF etching to improve fill factors from typically 64% to 72%. While we do not consider this method an acceptable production process, we do feel it is indicative of the results one can obtain with proper firing profiles, and that our limitation was strictly in the mechanics of the furnace used for firing.

The question of a back surface field (BSF), and specifically the use of a printed Al ink and fire-in were also briefly addressed. Several of the wafers were printed with TFS Al ink #5540 and fired at 800C for 4 minutes. Following a clean up, they were printed with the Ag/Al ink that was routinely used, and fired with wafers that did not have the Al applied prior to firing. The resultant cells were identical in all respects, including the open circuit voltage of 581 mV. While no BSF appeared to be present, the quality of the material (as discussed in previous sections) was suspect and may have limited these results because of low minority carrier diffusion lengths. For the remainder of the samples no separate Al print and fire was performed.

The parameters defined in the development stages were then used on the "production run" of over 100 wafers. These parameters had resulted in best cell efficiencies (without AR coating) of 8.7% on laser annealed wafers. This run as discussed previously, was necessary to generate the process statistics. The parameters for firing were as follows:

---

*Thick Film Systems, Santa Barbara, CA.

Print back ink, TFS #G505 or #3398

Dry back contact, 10 minutes at 120°C under heat lamp

Fire back contact, 4 minutes at 800°C in air atmosphere

Print front grid, ink TFS #3349

Dry front contact, 5 minutes at 120°C

Fire front contact, 1 minute at 725°C (setting), IR belt furnace

Test

The wafers left for the demonstration experiment (Section 4) were principally the wafers which were annealed with a "hot-spot" (lot #4636, Figure 10). These 64 wafers were processed and the final results were tabulated. These results are summarized in Table 6 along with the other cells processed. The results of a brief HF etch (5% solution for 3 seconds) are also presented for 29 cells from the first lot #4636. Two other small lots, #4642 and #4643 were also processed, and results from these lots after HF etching are presented. The last entry, lot #4638 are the furnace annealed "control" samples.

TABLE 6. AVERAGED PERFORMANCE OF LASER ANNEALED CELLS WITH SCREEN PRINTED CONTACTS

LOT #	SAMPLES	V_{oc}	J_{sc}	FF	EFFICIENCY
4636	64	.582	19.6	63%	7.2%
4636e	29	.582	20.6	67%	7.8%
4642	20	.581	19.9	71%	8.2%
4643	10	.574	19.7	72%	8.4%
4638	10	.583	21.2	71%	8.8%

During the processing of the wafers, no samples were broken.

3.6 POLYCRYSTALLINE CELL PROCESSING

Polycrystalline SILSO material was also processed using the above described production sequence. The resulting cell performance data are listed in Table 7. The mean variation in results was much greater than for single crystal material as might be expected. Variations in firing temperature by 25°C had no discernable effect. The grid pattern used is shown in Figure 11 for the finished SILSO cell. Two cells were also processed which had not received an anneal. The attempt was made to find whether or not the anneal could be done in-situ as part of the metallization process. Initial results looked quite promising as indicated in the following:

Laser Annealed Silso:	5.7% average efficiency
	6.1% best efficiency
Thermal Annealed Silso:	5.2% average efficiency
	5.6% best efficiency

No AR coatings were applied. One wafer broke during processing, due to the bowing of the wafers during the back metallization firing.

TABLE 7. DEMONSTRATION EXPERIMENT: Screen Printed Contacts on Laser Annealed Polycrystalline Material

Cell ID	V_{oc} (mV)	J_{sc} (mA/cm^2)	FF (%)	Efficiency (%)
2	494	16.9	61.3	5.1
3	501	16.8	64.9	5.5
4	508	17.8	69.2	6.1
5	504	16.3	70.0	5.8
6	511	17.1	71.7	6.3
8	511	16.7	69.8	5.9
9	506	16.8	64.8	5.5
12	499	17.2	64.7	5.5
13	506	17.7	65.9	5.9
14+	506	16.3	63.6	5.2
15*	495	16.8	58.5	4.9
16*	509	17.1	63.8	5.6

No AR coating.

\+ All cells 100 cm^2, except 14 (chipped) uncorrected.

* Cell 15 and 16 unannealed except for firing furnace treatment of screen printed contacts.

SECTION 4
DEMONSTRATION

4.1 DEMONSTRATE PROCESS AT PRODUCTION SPEED

The objective of this task was to demonstrate the ability of the chosen laser to implement the selected process. The data was used to calculate the throughput for the cost estimates of a production line presented in Section 5.

The throughput was originally estimated at 600 wafers per hour with 80% uptime. This value is limited by the ion-implanter capabilities. With the possibility that a reduced ion-dose may be acceptable, the throughput estimates were increased to 700 wafers per hour to match the rest of the production line. The chosen laser must be able to anneal a 100 mm wafer (round or square) in a time between 5.14 and 6.43 seconds to meet this throughput requirement.

The test was witnessed by a JPL observer. The scanning pattern for annealing is shown in Figure 5 along with the time required to complete each leg of the pattern. The laser successfully annealed the wafer with a 10 cm/sec velocity, 150 Hz repetition rate, a 330 mJ pulse energy, and a beam width of 0.6 mm. The total time for motion is 5.5 seconds. However, the time required for acceleration, deceleration, and a pause for relay trip time at the end of each motion step added 0.5 second for each line scanned by the motorized x-y table, bringing the total processing time to 7.5 seconds. This time can be reduced by using either continuous motion or by better table driving electronics.

The demonstrated processing throughput capability of the Questek 2260 excimer laser exceeds 25 cm^2/sec with 50 watts of light output at 248 nm, providing the dead time can be reduced to zero. The dead time is that period during beam scanning when the laser is not usefully annealing material. For example, the dead time shown in Figure 5 is 1.5 seconds (plus the time required to load and unload the scanning table). For production purposes it is assumed that the wafers will be moving on a continuous belt from a cassette unloader to the front contact screen printer. The laser beam can then be rastered over the surface of the moving wafer by a beam scanner using rotating mirrors. This reduces

loading/unloading dead time for a production annealing system to zero. Because rotating mirrors have much higher acceleration and ultimate velocity compared to the 10 kg translating table, the 1.5 second dead time in Figure 5 can be reduced to less than 0.4 seconds for even the slowest typical scanners.* The question is whether the beam focus can be maintained for such a large spot size when the true distance between the laser and sample varies using rotating mirrors. New compensating optics with dynamic focussing adjustments* combined with a large tolerance for focussing error (see Figure 8) can maintain the beam quality, and the throughput desired.

4.2 DEMONSTRATE PRODUCT

The objective of this task was to produce a quantity of product using pulsed excimer laser processing to estimate the actual efficiency and yield of this process in a production environment. Due to a delay in developing an adequate screen printed contact procedure the wafers used for this demonstration experiment were split into two groups; 100 wafers (plus controls) received screen printed contacts and 92 additional wafers (plus controls) received fine-line evaporated contacts.

The material comprised Monsanto CZ silicon with a specified resistivity of 1 to 5 ohm-cm, 100 mm diameter wafers with a polished front surface and a lapped back surface finish. These wafers were cleaned, but not etched, implanted with phosphorus to a dose of 2.5×10^{15} ions/cm^2 using the SPI-ION™ 1000. The dose uniformity at implant was estimated to be better than $\pm 10\%$, across each wafer and from wafer-to-wafer. The material was stored in a nitrogen atmosphere until just before laser annealing. The laser parameters were 248 nm light at 400 mJ per pulse at a repetition rate of 20 Hz. The beam width was 0.7 mm and the estimated fluence was 1.65 J/cm^2 when illumination was uniform.

*General Scanning Inc., Watertown, MA

After laser annealing the wafers were cleaned again and contacts applied. The screen printed contact process was described in Section 3.5. Evaporated Ti-Pd-Ag contacts were defined by photoresist. After lift-off and sintering at 400°C the contacts were plated to a 10 μm line thickness. Large area cells (53 cm^2), shown in Figure 13, were then cut from the wafer and measured. The shaded area for fine-line contacts was 3%, and for screen printed contacts it was 8%. A few cells from both groups had AR coatings applied. In all cases the maximum power output was increased by a factor of 1.40 after AR coatings were applied.

Solar cell results for this demonstration experiment with screen printed contacts are presented in Table 8. Solar cell results with fine-line evaporated contacts shown in Figure 13 are presented in Table 9 for the demonstration experiment. The difference in average maximum power for the two groups of cells, neglecting surface damaged cells, is entirely consistent with extra metal coverage by screen printed contact pattern, and the lower fill factor of the screen printed pattern (attributed to ink problems). This implies that the PELA process is consistent with screen printed contacts on polished or bright etched surfaces.

Results are summarized in Table 10. The average efficiency will be used in the economic analysis (Section 5). No wafers were lost during the laser annealing process. Automated equipment could easily detect the scattered light generated when the wafer surface is damaged and this would avoid the electrical yield loss noted in this experiment. Therefore, yield loss during PELA will be limited to typical wafer breakage rates with automated equipment.

TABLE 8. DEMONSTRATION EXPERIMENT: SCREEN PRINTED CONTACTS ON LASER ANNEALED WAFERS

CELL ID	no HF etch V_{oc} (mV)	J_{sc} (mA/cm^2)	F.F. (%)	Eff. (%)	after HF etch V_{oc} (mV)	J_{sc} (mA/cm^2)	F.F. (%)	Eff. (%)
36-01	575	18.6	57.9	6.2	582	20.1	65.9	7.7
36-02	578	20.1	59.8	6.9	579	20.3	67.8	8.0
36-03	581	19.8	60.7	7.0	582	20.8	63.0	7.6
36-04	582	19.6	61.1	7.0	584	20.6	20.6	7.7
36-05	582	19.9	64.0	7.4	584	20.5	67.1	8.0
36-06	583	19.9	64.2	7.4	584	21.3	65.0	8.1
36-07	580	20.1	55.6	6.5				
36-08	583	19.8	65.0	7.5	584	20.4	67.1	8.0
36-09	581	20.0	64.2	7.5	583	20.3	67.9	8.0
36-10	578	19.4	58.0	6.5				
36-11	579	19.4	63.0	7.1	581	20.9	66.3	8.1
36-12	583	19.4	65.0	7.3				
36-13	580	19.3	62.1	6.9				
36-14	581	19.6	63.4	7.2	582	20.8	67.4	8.2
36-15	585	19.1	63.9	7.2				
36-16	582	19.6	62.8	7.2	583	20.5	69.1	8.3
36-17	584	19.6	65.0	7.4				
36-18	582	19.5	64.3	7.3				
36-19	587	19.7	67.8	7.9				
36-20	583	19.7	62.1	7.1				
36-21	585	19.7	65.4	7.5				
36-22	585	19.5	64.8	7.4				
36-23	580	19.5	58.7	6.6				
36-24	584	19.5	64.6	7.3				
36-25	583	19.4	65.5	7.4				

No AR coating.

All cells 78 cm^2 (100 mm diameter).

All cells 36-xx had surface damage.

TABLE 8. DEMONSTRATION EXPERIMENT: SCREEN PRINTED CONTACTS ON LASER ANNEALED WAFERS (continued)

CELL ID	no HF etch V_{oc} (mV)	J_{sc} (mA/cm^2)	F.F. (%)	Eff. (%)	after HF etch V_{oc} (mV)	J_{sc} (mA/cm^2)	F.F. (%)	Eff. (%)
36-26	580	19.9	58.7	6.8	578	19.8	66.8	7.6
36-27	584	19.5	66.5	7.6	582	19.6	66.5	7.6
36-28	581	19.6	62.7	7.1	581	19.9	67.0	7.7
36-29	584	19.9	61.7	7.2	583	-	-	7.6
36-30	582	19.2	62.4	7.0	581	19.8	66.4	7.6
36-31	583	19.2	65.2	7.3	582	20.0	66.9	7.8
36-32	583	19.3	63.4	7.1	582	20.2	66.8	7.9
36-33	584	20.0	62.5	7.3	583	20.0	69.0	8.1
36-34	583	19.9	63.6	7.4	579	-	-	7.5
36-35	581	19.5	64.1	7.2	582	20.3	65.1	7.7
36-36	581	19.3	64.8	7.3	581	20.0	68.1	7.9
36-37	583	19.7	66.9	7.7	582	19.9	68.0	7.9
36-38	584	19.3	64.9	7.3				
36-39	585	19.4	66.1	7.5				
36-40	579	19.1	60.8	6.7				
36-41	580	19.5	60.5	6.8				
36-42	582	19.3	64.3	7.2	582			7.6
36-43	582	19.6	63.0	7.2				
36-44	578	19.4	59.2	6.6	579	20.2	62.4	7.3
36-45	581	19.6	65.9	7.5	582	-	-	8.1
36-46	587	20.4	63.3	7.6	587	20.5	67.8	8.2
36-47	582	19.0	63.7	7.0		-	-	
36-48	585	19.8	64.3	7.5	586	-	-	8.2
36-49	586	20.2	65.5	7.7	585	20.7	67.4	8.2

No AR coating.

All cells 78 cm^2 (100 mm diameter).

All cells 36-xx had surface damage.

TABLE 8. DEMONSTRATION EXPERIMENT: SCREEN PRINTED CONTACTS ON LASER ANNEALED WAFERS (continued)

CELL ID	no HF etch V_{oc} (mV)	J_{sc} (mA/cm^2)	F.F. (%)	Eff. (%)	after HF etch V_{oc} (mV)	J_{sc} (mA/cm^2)	F.F. (%)	Eff. (%)
36-76	565	19.0	56.1	6.0				
36-77	576	19.1	65.9	7.3				
36-78	572	19.2	64.4	7.1				
36-79	570	19.4	65.4	7.3				
36-80	568	19.5	62.7	6.9				
36-81	572	18.9	65.4	7.1				
36-82	565	18.3	63.5	6.5				
36-83	575	19.2	59.6	6.6				
36-84	569	19.5	62.0	6.9				
36-85	568	19.3	62.5	6.8				
36-86	567	18.9	60.8	6.5				
36-87	568	19.2	67.9	7.4				
36-88	572	18.8	67.9	7.3				
36-89	572	19.0	71.6	7.8				
36-90	576	18.9	74.0	8.0				
36-91					572	18.9	64.7	7.0
36-92					575	19.1	72.6	8.0
36-93					576	19.0	72.9	8.0
36-94					571	19.3	72.0	7.9
36-95					575	19.4	72.0	8.0
36-96					575	19.8	70.0	8.0
36-97					572	18.9	72.4	7.8
36-98					573	19.4	69.6	7.7
36-99					575	19.9	70.9	8.1

No AR coating.

All cells 78 cm^2 (100 mm diameter).

All cells 36-xx had surface damage.

TABLE 8. DEMONSTRATION EXPERIMENT: SCREEN PRINTED CONTACTS ON LASER ANNEALED WAFERS (concluded)

CELL ID	no HF etch V_{oc} (mV)	J_{sc} (mA/cm^2)	F.F. (%)	Eff. (%)	after HF etch V_{oc} (mV)	J_{sc} (mA/cm^2)	F.F. (%)	Eff. (%)
42-24	583	19.8	73.1	8.4				
42-25	582	19.7	73.3	8.4				
42-26	577	19.5	70.1	7.9				
42-27	582	20.0	71.3	8.3				
42-28	578	19.7	68.9	7.9				
42-29	584	19.5	69.7	7.9				
42-30	582	20.0	70.1	8.2				
42-31	581	19.8	66.5	7.6				
42-32	582	20.0	71.8	8.4				
42-33	582	19.6	69.4	7.9	slight surface			
42-34	584	19.6	70.5	8.1	damage (variable)			
42-35	583	20.0	71.1	8.3				
42-37	578	19.5	66.4	7.5				
42-39	582	19.7	74.8	8.6				
42-40	581	19.8	74.1	8.5				
42-41	580	19.9	72.9	8.4	no surface			
42-42	580	20.2	71.3	8.4	damage			
42-43	582	19.9	72.5	8.4				
42-44	578	20.7	70.2	8.4				
42-45	580	20.5	71.0	8.5				
37-26	580	19.9	70.9	8.2				
37-50	580	20.2	72.7	8.5				
38-9	586	21.2	71.9	8.9				
38-10	579	21.2	68.6	8.4				
38-11	584	21.5	71.4	9.0				
38-12	584	21.2	70.8	8.8	Furnace			
38-13	585	21.6	71.3	9.0	Annealed			
38-14	585	21.4	71.3	8.9				
38-24	583	21.6	71.4	9.0				
38-25	583	21.7	71.2	9.0				
38-35	582	19.5	74.5	8.5				

No AR coating. All cells 78 cm^2 (100 mm diameter). All cells 36-xx had surface damage.

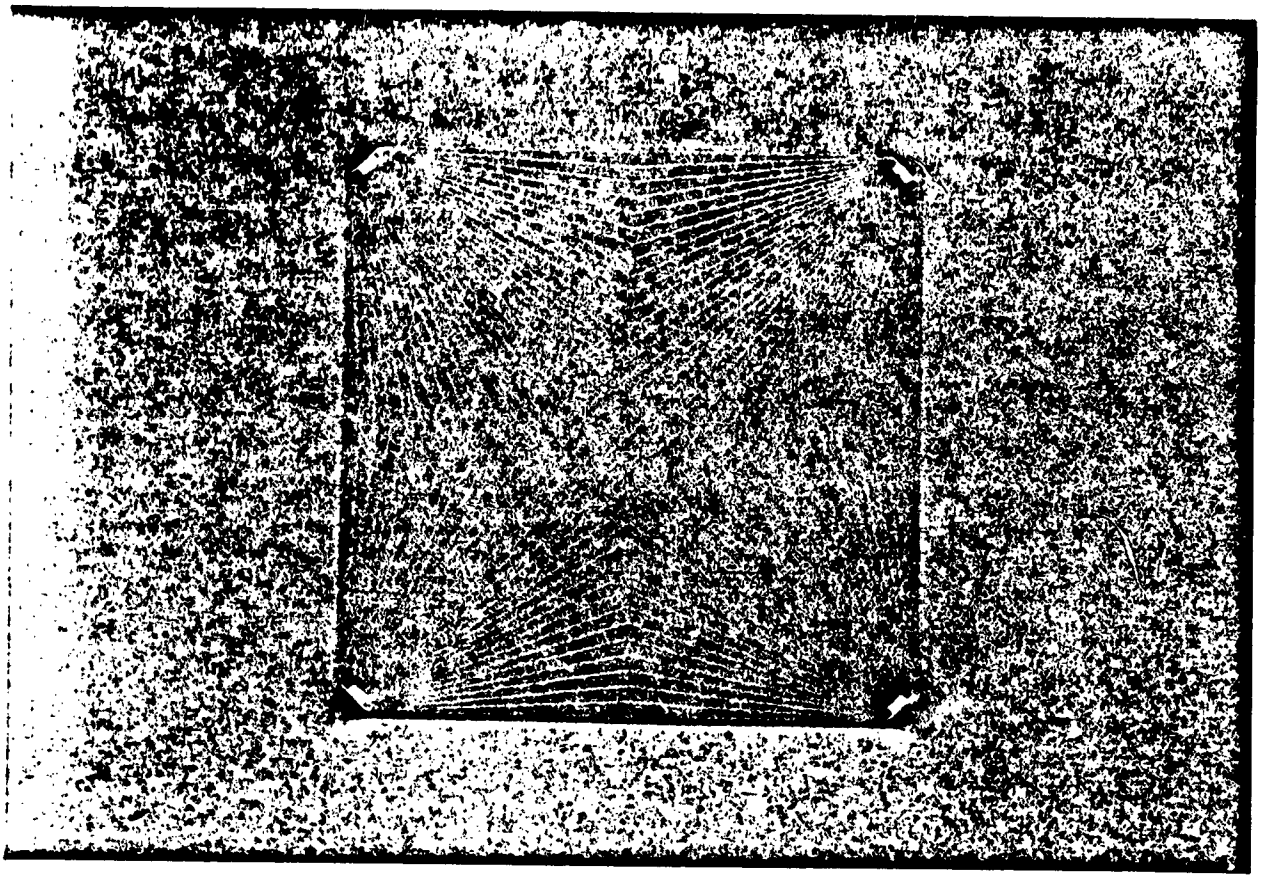

FIGURE 13. EVAPORATED CONTACT PATTERN ON 53 cm^2 CELL.

TABLE 9. DEMONSTRATION EXPERIMENT: EVAPORATED CONTACTS ON LASER ANNEALED CELLS

CELL ID	V_{oc} (mV)	J_{sc} (mA/cm^2)	F.F. (%)	Eff. (%)
37-26	582	22.2	77.7	10.1
37-27	576	18.6	83.4	9.0
37-28	586	22.0	78.3	10.1
37-29	582	+	+	10.0
37-30	587	21.7	78.8	10.0
37-31	587	22.0	78.4	10.1
37-32	578	21.1	77.9	9.5
37-33	585	22.2	78.1	10.1
37-34	580	21.1	78.4	9.6
37-35	582	21.4	78.7	9.8
37-36	581	21.8	78.7	10.0
37-37	578	21.7	78.3	9.8
37-38	579	21.3	77.0	9.5
37-39	576	21.2	77.9	9.5
37-40	576	21.5	78.3	9.7
37-41	581	21.1	79.6	9.7
37-42	579	21.8	77.7	9.8
37-43	579	21.8	78.7	9.9
37-44	579	21.7	77.4	9.7
37-45	579	21.3	79.4	9.8
37-46	581	21.4	74.0	9.2
37-47	581	21.8	76.6	9.7
37-48	580	21.5	80.0	10.0
38-15	584	22.3	77.0	10.0*
38-16	584	22.0	78.7	10.1*

* Furnace Annealed control. First lot of 25 wafers processed together.

\+ Data lost. All cells 53 cm^2, no AR coating.

TABLE 9. DEMONSTRATION EXPERIMENT: EVAPORATED CONTACTS ON LASER ANNEALED CELLS (continued)

CELL ID	V_{oc} (mV)	J_{sc} (mA/cm^2)	F.F. (%)	Eff. (%)
37-51	578	20.9	78.4	9.5
37-54	576	21.1	77.5	9.4
37-55	579	21.0	78.8	9.6
37-56	569	19.6	72.1	8.1
37-58	581	20.8	78.3	9.5
37-59	580	21.0	78.5	9.6
37-60	580	21.2	78.4	9.7
37-61	583	20.8	78.7	9.6
37-62	578	21.3	78.2	9.6
37-63	581	21.4	78.0	9.7
37-64	582	21.2	78.7	9.7
37-65	580	21.0	77.8	9.5
37-66	579	21.3	78.9	9.7
37-67	576	20.7	78.6	9.4
37-68	577	20.3	78.3	9.2
37-69	580	21.0	78.6	9.6
37-70	579	21.0	76.9	9.4
37-71	581	21.3	77.9	9.6
37-72	584	21.1	78.6	9.7
37-73	577	20.9	78.8	9.5
37-74	577	21.0	76.9	9.3
37-75	579	20.5	78.2	9.3
38-77	573	20.4	75.5	8.8
38-17	580	21.5	76.5	9.5*
38-18	582	21.9	76.9	9.8*

* Furnace annealed control.

Second lot of 25 wafers processed together.

TABLE 9. DEMONSTRATION EXPERIMENT: EVAPORATED CONTACTS ON LASER ANNEALED CELLS (continued)

CELL ID	V_{oc} (mV)	J_{sc} (mA/cm^2)	F.F. (%)	Eff. (%)
37-78	575	21.5	77.1	9.5
37-79	578	21.6	77.8	9.7
37-80	578	21.8	77.5	9.7
37-81	578	21.5	78.2	9.7
37-82	579	21.5	78.3	9.7
37-83	575	21.2	77.8	9.5
37-85	579	21.8	78.3	9.9
37-86	580	21.3	76.5	9.4
37-87	580	21.0	77.8	9.5
37-88	582	21.4	77.5	9.6
37-89	577	21.2	78.3	9.6
37-90	580	21.5	78.8	9.8
37-91	580	21.6	78.2	9.8
37-92	583	21.5	78.4	9.8
37-93	576	21.5	78.1	9.7
37-94	581	21.5	78.3	9.8
37-95	579	21.7	76.9	9.7
37-96	576	21.0	77.0	9.3
37-97	578	21.5	78.2	9.7
37-98	576	21.5	77.9	9.7
37-99	577	21.4	78.2	9.7
37-100	577	21.1	78.0	9.5
38-19	579	21.8	76.7	9.7*
38-20	582	22.2	76.9	9.9*

* Furnace annealed control.

Third lot of 25 wafers processed together (one lost to breakage).

TABLE 9. DEMONSTRATION EXPERIMENT: EVAPORATED CONTACTS ON LASER ANNEALED CELLS (concluded)

CELL ID	V_{oc} (mV)	J_{sc} (mA/cm^2)	F.F. (%)	Eff. (%)
42-1	578	21.0	78.0	9.5
42-2	580	20.9	77.7	9.4
42-3	579	20.9	78.3	9.5
42-4	581	21.0	77.8	9.5
42-5	579	20.9	78.9	9.5
42-6	581	21.0	78.1	9.5
42-7	580	20.8	78.7	9.5
42-8	580	21.0	78.6	9.6
42-9	581	20.9	78.7	9.6
42-10	581	20.9	77.3	9.4
42-11	580	21.1	77.5	9.5
42-12	577	20.8	78.3	9.4
42-13	576	20.6	78.3	9.3
42-14	582	21.2	78.2	9.6
42-15	581	21.2	77.8	9.6
42-16	580	21.2	78.3	9.7
42-17	577	20.3	78.4	9.2
42-18	581	21.3	78.1	9.6
42-19	580	21.2	77.9	9.6
42-20	578	21.0	78.6	9.5
42-21	577	21.0	77.7	9.4
42-22	580	21.1	78.8	9.6
38-23	581	21.2	78.7	9.7
38-21	581	22.1	76.7	9.8*
38-22	581	21.5	76.9	9.6*

* Furnace annealed control.

Fourth lot of 25 wafers processed together.

TABLE 10. SUMMARY OF RESULTS FOR DEMONSTRATION EXPERIMENT (Non AR coated)

Lot #	# Samples	V_{oc} (mV)	J_{sc} (mA/cm^2)	FF (%)	Eff. (%)
A (best sample)	25	581 (2) 528	19.9 (0.3) 19.7	71 (2) 74.8	8.2 (0.3) 8.6
B (best sample)	75	582 (2) 587	20.6 (0.3) 20.5	66(2) 69	8.0 (0.2) 8.3
C (best sample)	10	583 (2) 583	21.2 (0.6) 21.6	71 (1) 71.4	8.8 (0.3) 9.0
D (best sample)	92	580 (3)	21.2 (0.3)	78.1 (.6)	9.6 (.2)
E (best sample)	8	582	21.7	77.0	9.8
F (best sample)	11	505 (7) 511	17.2 (1) 17.1	65 (3.8) 71.7	5.7 (0.5) 6.3

A: Laser annealed without surface damage, with screen printed contacts.
B: Laser annealed with minor surface damage and screen printed contacts.
C: Furnace annealed with screen printed contacts.
D: Laser annealed with fine-line evaporated contacts.
E: Furnace annealed with fine-line evaporated contacts.
F: Polycrystalline silicon, laser annealed with screen printed contacts.

The furnace annealing control results presented in Table 10 are considered below average for this processing sequence at Spire Corporation. An average efficiency of 10.7 percent without AR coatings would be expected. The discrepancy is related to the lapped and unetched back surface of the wafers. The proposed production sequence (Section 5) would etch both sides of the wafers.

4.3 EVALUATION OF PELA SOLAR CELLS

Data presented in Table 11 indicate that the furnace annealed control cells were more efficient than laser annealed cells for identical processing. This is opposite to results expected at the start of the program. Additional tests were performed to explain the observed differences.

Figure 14 shows the measured quantum efficiency of large area cells with fine-line evaporated contacts. The PELA cells show reduced blue response with nearly identical red response. The response at long wavelengths implies large minority carrier lifetime in both cells. In particular, the three step furnace anneal used (550°C for one hour, ramp up to 850°C, hold for 15 minutes, ramp down to 550°C and hold for one hour) did not degrade the minority carrier lifetime relative to the low temperature PELA process. The poor blue response of the PELA cell is attributed to excess light absorption in the emitter as explained below.

The sheet resistance of PELA wafers was typically 40 ohms per square compared to 80 to 100 ohms per square for furnace annealed wafers with the same ion-implant (2.5×10^{15} ions/cm^2 at 10 keV, phosphorus). The PELA process is expected to activate nearly 100% of the implanted dopant which implies that the furnace anneal activated only about 50% of the dopant.[11] This was confirmed by the direct measurements of the dopant profiles.

Dopant profiles were determined by spreading resistance measurements shown in Figure 15. The junction depths for the PELA process used here and for the furnace anneal are nearly identical for the case of evaporated contacts sintered at low temperatures. The total active concentration of phosphorus in the furnace annealed material is smaller than that in the laser annealed material. The maximum concentration of phosphorus in the PELA sample (2×10^{20}/cm^3) is near the maximum solid solubility limit at room temperature. PELA processing can activate dopant concentrations in excess of this limit,[11] but with excess light absorption.[12] These data explain the blue response in Figure 14, the lower short circuit current density (J_{sc}) by sample D compared to sample E in Table 10, and the better fill factor (FF) of sample D compared to sample E.

The PELA cell with evaporated contacts was exposed to no temperatures over 400°C after annealing, so that the dopant profile shown in Figure 15 represents the profile directly after annealing. Screen printed contacts were fired at higher temperatures, up to 750°C, and this was sufficient to diffuse the phosphorus to some extent as shown in Figure 15. The peaking of the phosphorus distribution at the cell surface for this case might be due to some oxide growth and gettering. Comparing samples A and C in Table 10, the fill factor for PELA cells with screen printed contacts was better than the fill factor with furnace annealed contacts, but the short circuit current density for PELA was lower, implying that excess light absorption may have been a problem.

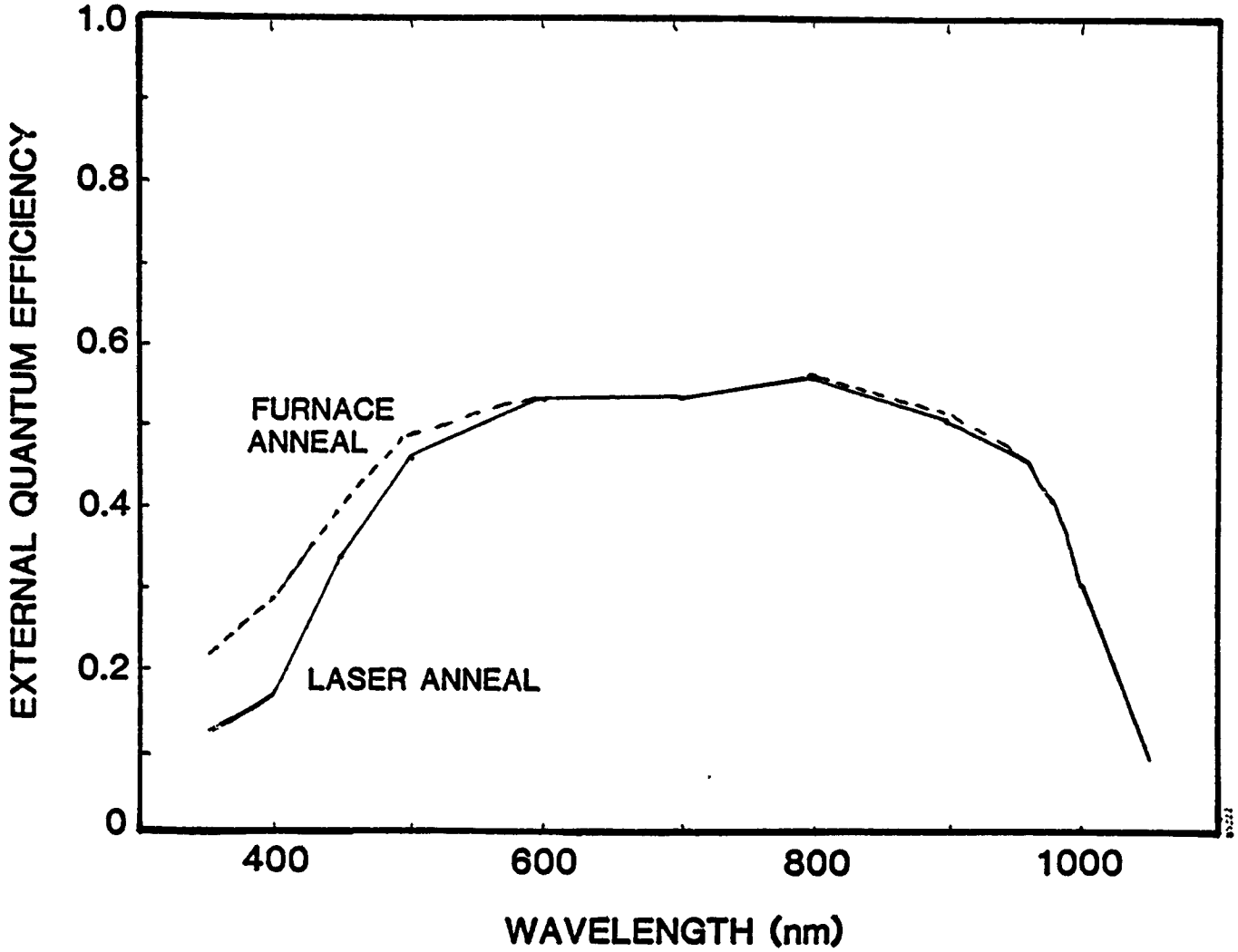

53cm^2 CELL
EVAPORATED CONTACTS

FIGURE 14. QUANTUM EFFICIENCY.

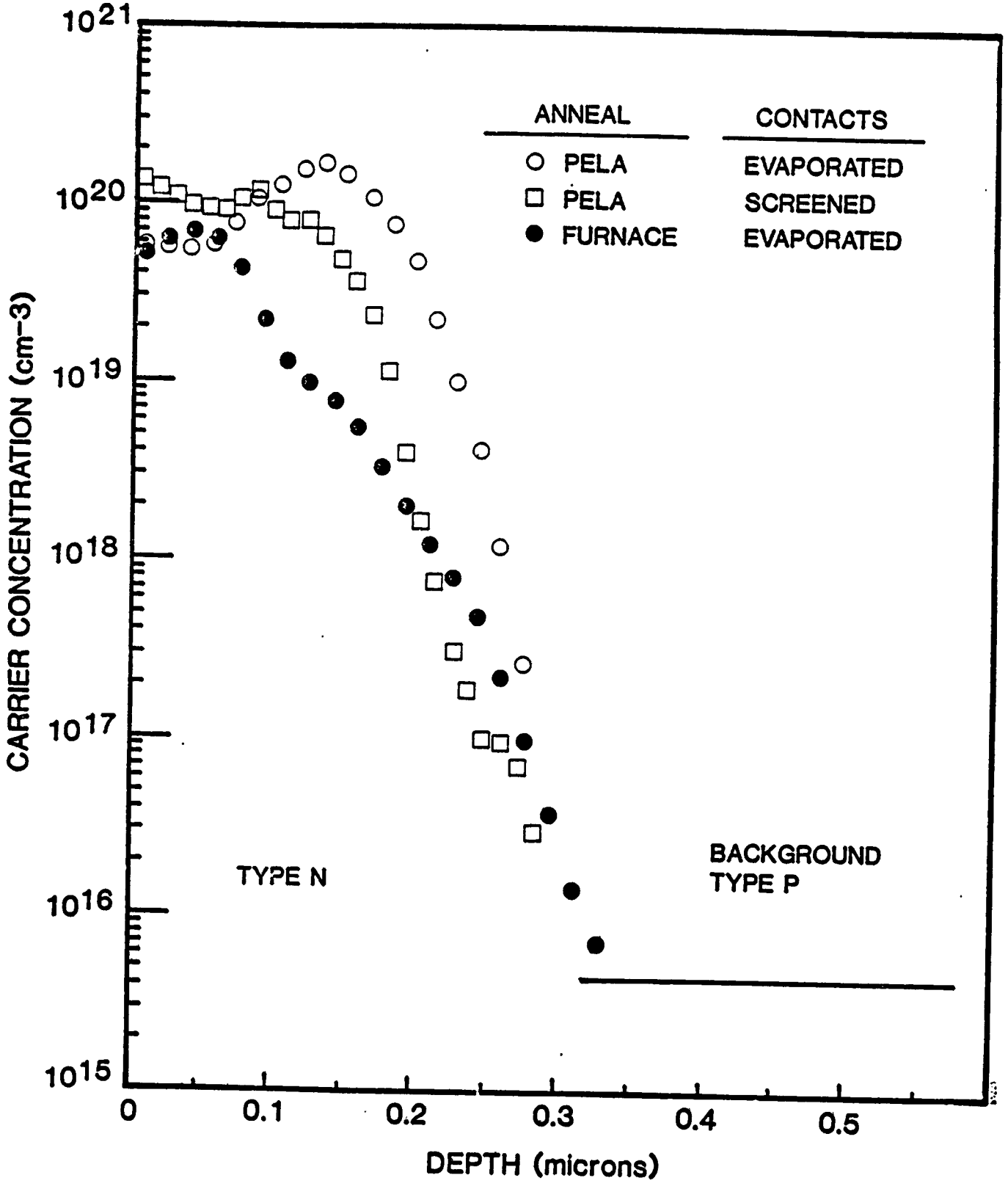

FIGURE 15. SPREADING RESISTANCE PROFILES.

The PELA results presented may have been improved by using lower ion implantation doses. This should improve the transmission of light through the emitter and improve blue response and short circuit current density while reducing the fill factor only slightly. This effect was never observed in previous PEBA[13] experiments where the doping profile differed and was discovered too late to obtain new cell data in this program.

SECTION 5
ECONOMIC ANALYSIS

The objective of this task was to estimate the cost of pulsed excimer laser annealing (the selected process in Section 2.1) to fabricate crystalline silicon solar cells. The estimates presented herein are based on the IPEG analysis developed by JPL,[14] supplemented by a SAMICS analysis[15] for the excimer laser processing step (Appendix).

The largest cost factor in pulsed excimer laser annealing (PELA) is ion-implantation. Annealing is a much less costly process. Therefore, the cost effectiveness of PELA must be judged in comparison to other thermal annealing processes as well as to the diffusion process. Total fabrication procedures are presented in Table 11. The three annealing procedures considered, and the diffused junction process are:

a) Pulsed excimer laser annealing
b) Furnace annealing with surface passivating oxide growth
c) Furnace annealing without surface passivating oxide growth
d) Diffusion of sprayed on dopant

Process (a) was developed during the course of this study. Process (b) is the high efficiency anneal process now used by Spire for other research programs[16] with appropriate simplification for production. Process (c) is a short-time high temperature anneal. The anneal cycle used for control samples in this program was similar to process (b) but without oxygen admitted to the annealing furnace. The cost for any thermal annealing cycle would lie between the estimates for (b) and (c), specifically chosen to represent the minimum (maximum) equipment and direct labor requirements conceivable. Process (d) is a comparable diffused junction process line with equal throughput.

Each of the four processes analyzed is based upon manufacturing equipment now offered by Spire Corporation. Prices and data for the module line are based on many units sold in a standard configuration. Equipment for the cell line is always customized for particular applications so that projected costs and yields may vary.

TABLE 11. PROCESS DEFINITION FOR IPEG ANALYSIS

(a) LASER ANNEAL	(b) FURNACE ANNEAL with surface passivating oxide	(c) FURNACE ANNEAL without passivation	(d) DIFFUSION
input as-cut wafers	input as-cut wafers	input as-cut wafers	input as-cut wafers
etch saw damage rinse bright etch HCl clean rinse dry	etch saw damage rinse texture-etch Hcl clean rinse dry	etch saw damage rinse texture-etch Hcl clean rinse dry	etch saw damage rinse texture-etch Hcl clean rinse dry
ion-implantation (non-mass analyzed phosphorous at 10 keV to 1.0-2.0x10^{15} ions/cm^2)	ion implantation	ion implantation	
laser anneal (while loading screen printer)	anneal tube furnace (1 hour)	belt furnace anneal (15 min)	spray-on dopant diffuse junction coin-stack plasmaetch HF clean rinse
print and dry back contact	—	—	
print and dry front contact	—	—	dry
AR coating by CVD	—	—	print and dry back contact
Solder dip clean test and sort (to module line)	— — — —	— — — —	print and dry front contact
			solder dip clean test and sort (to module line)

The KrF laser was chosen for the production line. The economics behind this decision are summarized in Table 12. Basically, a 50 watt KrF laser is smaller than a XeCl excimer laser with equal output because the conversion efficiency of the former is greater (3% compared to 2%). The KrF laser needs more frequent gas changes but fewer spare parts. It is judged to be the lower risk alternative as a standard Questek laser with KrF demonstrated 50 watt output (Section 5.1). Complete Samics input for this process is included in Appendix B.[15]

TABLE 12. COMPARISON OF OPERATING COSTS FOR 50 WATT KrF AND XeCl LASERS

ITEM	KrF	XeCl
Capital Cost + spare parts (x 0.59)	$37,760.	$47,200.
Annual Replacement Parts (3 shifts at 1850 hours each) (x 1.17) at 80% duty cycle	51,597.	73,242.
Anneal Gas Cost (x 1.17)	(Fill every 2 hours) 61,196.	(Fill every 8 hours) 41,155.
Total (estimated annual operating cost)	$150,553.	$161,597.

Notes: Direct operating labor identical, slightly higher maintenance labor for XeCl laser. Also, slightly higher utilities usage for XeCl laser. These figures small compared to above totals.

The IPEG formula used to calculate the total cost is:

Total cost = 0.59 x capital equipment price
+ $136 x area (sq. ft.) to operate equipment
+ 2.02 x direct labor cost
+ 1.17 x materials cost
+ 1.17 x utilities cost

The price for capital equipment was estimated to be the 1985 manufacturers' list price. The direct labor cost was estimated to be either $5.00, $7.50, or $10.00 per hour depending upon the skill of the technician required. The materials costs are based upon 1985 estimates from suppliers. The utilities costs were estimated as $93 per kW hr per year, $0.00038 per gallon of cooling water, and $100.00 per 1000cfm of exhaust air per shift.

The production line was assumed to run three shifts per day, each shift is 1850 hours per year. The uptime for the ion-implanter was estimated at 80% and was assumed to be the gating maintenance requirement. The average uptime of any other piece of equipment was assumed not to affect total factory throughput. The average uptime of the diffused process line was assumed to be 85%. The total yield for each of the four processes was assumed to be equal at 90%, but this figure will be discussed in more detail. The maximum processing rate for much of the equipment manufactured by Spire Corporation is listed at 700 wafers (100 mm diameter) per hour. This was assumed to be the processing rate for <u>all</u> equipment. The total number of wafers started (major materials cost at $3.25 each assumed) is therefore 1850 hours/year x 3 shifts x 700 wafers/hour x 0.80 uptime = 3,108,000 (or 3,496,500 at .85 uptime for process d). The total production is 90% of this figure (times wafer area x 100 mw/cm^2 x efficiency) and varies with different process efficiencies. Although the yield loss is distributed throughout the cell and module lines the total materials use at all fabrication steps is based on processing the total 3,108,000 wafers. A detailed breakdown for the requirements of each process step is given in Table 13.

A summary of the economic calculation is presented in Table 14. The cost per wafer to fabricate a completed module is based upon the assumptions given above and Table 11. The efficiencies given are extrapolated for screen printed contacts on AR coated wafers. The numbers for processes (a) and (c) were derived by multiplying the efficiency given in Table 6 for fine-line contacts by 1.40 (AR coating), then multiplying by 0.95 for excess metal coverage with screen printed contacts, finally multiplying by the ratio of expected fill factor to fill factor with evaporated contacts (0.75/0.78). The efficiencies calculated this way are conservative. The efficiency for process (b) uses the actual numbers for cells fabricated for high efficiency modules delivered to JPL (contract number 956641) of 15.5% and derates this figure by 0.95 x (0.75/0.78) as described above. The efficiency for processes (d) is the guaranteed minimum for this line.

TABLE 13. REQUIREMENTS FOR EACH PROCESS STEP

1) As-cut silicon wafers, cleaned from saw slurry ($3.25 wafer)

2) Damage Removal

SPI-ETCH 500: $32,000
Cassette loader: $25,000
Area: 104 $ft.^2$
Electricity: 4 kW average
Nitrogen: 400 slm
Exhaust: 1000 cfm
Deionized water: 1 gal/wafer (40 liters /min, 3¢/wafer)
NaOH: pellets for 20% molar solution, 0.3¢/wafer
Direct labor: 1 person at $5

3(a) HCl clean (no texturing)

(additions to units in step 2)
SPI-CLEAN 2000: $29,500
Area: 80 Ft^2
Electricity: 3 kW
N_2: 400 slm
Exhaust: 1000 cfm
HCl: 1cc/wafer, or 1.25¢/wafer
Direct labor: 1 at $5/hr.
Spare parts: Per year, (3a,b,c,d,) $12,000

3(b,c, d) Texture Etch

(additions to units in step 2)
SPI-ETCH 500: $32,000
Area: 104 ft^2
Electricity: 4 kW
N_2: 400 slm
Exhaust: 1000 cfm
NaOH: (10% of cost in item 1, 0.03¢/wafer)
HCl: 1 cc/wafer
Direct labor: 1 @ $5/hr.

TABLE 13. REQUIREMENTS FOR EACH PROCESS STEP (continued)

4) Ion Implantation

SPI-ION™1000: $600,000
Area: 168 ft^2
Electricity: 10 kW
Cooling water: 1 gpm
Liquid N_2: 100 liters/8 hours
Phosphorus: $5/8 hours
Spare parts: $30,000/year
Direct labor: 1 at $10/hour
Exhaust: 100 cfm

4(d) Spray-on Dopant and Diffusion

Cassette-to-belt transfer: $23,250
Belt sprayer: $50,000
Belt-to-belt transfer: $22,000
Diffusion Furnaces (2): $60,000 each
Belt-to-stacker transfer: $15,000
Area: 400 sq. ft.
Dopant: $ .01/wafer
Electricity: 97 kW
Nitrogen: 150 slm
Air: 1250 slm
Exhaust: 2500 cfm
Cooling water: 10 gpm
Labor: 2 @ $5/hour
Spare parts @ $500/yr.

TABLE 13. REQUIREMENTS FOR EACH PROCESS STEP (continued)

5(a) Laser Anneal

50 watt Questek Laser: $65,600
Area: 40 ft.^{2} Scanner: $8,300
Spare parts: $20,000/shift/year
Electricity: 5 kW
Cooling water: 2 gpm
Kr: $16/fill
F_2: $0.68/fill 4 fills/shift, 1.3¢/wafer
He: $2.00/fill
Liquid N_2: 10 liters/shift, $0.37/liters
Labor: 0.1 tech @ $10/ hour

5(b) Furnace Anneal w/Passivating Oxide

Furnace, 4 tubes, autoload: $120,000
Automatic boat-to-cassette transfer robot: $30,000
Area: 150 ft.^{2} (15 x 10)
Electricity: 20 kW (5 kW/tube)
Nitrogen: 5 slm/tube
Cooling Water: 2 gpm
Exhaust air: 500 cfm
Direct labor: 1 @ $5/hour
Spare parts: $1000/month/shift

5(c) Annealing Belt Furnace

Furnace: $53,800
Area: 143 ft.^{2} (13 x 11)
Electricity: 15 kW
Nitrogen: 200 slm
Exhaust: 1000 cfm
Cooling water: 2 gpm
Direct labor: -0-
Spare parts: $5,400

TABLE 13. REQUIREMENTS FOR EACH PROCESS STEP (continued)

5(d) Coin-stack Etch and HF Etch

Plasma etcher: $25,000
Stacker to cassette transfer: $25,000
SPI-ETCH (HF): $30,000
Area: 250 sq. ft.
Electricity: 5 kW
Nitrogen: 500 slm
HF: $.001/wafer
DI water: 1 gal/wafer $.03/wafer
Exhaust: 1000 cfm
Spare parts: $1100/year
Direct Labor: 1 @ $5/year

6) Print and Dry Back Contact

[5a) goes between IR dryer and belt unloader]
Semi-automatic screen printer: $70,000
Cassette loader from belts: $19,500
IR drying furnace: $17,200
Area: 110 $ft.^2$
Al doped ink, 0.4g/wafer @ $0.55/g, 22¢/wafer
Solvent, screens, etc.: $1,000/month/shift
Spare parts for furnace: $2,000/year
Electricity: (1 kW + 12 kW)
Cooling water: none
Exhaust air: 1000 cfm
Compressed air: (clean, dry) 100 s/m
Direct labor: 2 @ $5/hour

TABLE 13. REQUIREMENTS FOR EACH PROCESS STEP (continued)

7) Print and Dry Front Contact

Semi-automatic screen printer: $70,000
Dryer & Firing furnace: $44,000
Belt-to-cassette transfer: $19,500
Area: 210 sq. ft.
Ag ink, 0.2g @ $0.55/g, 11¢/wafer
Solvent, screens, etc.: $1,000/month/shift
Spare parts for furnaces: $7,500/yr
Electricity: 28 kW
Cooling water: 2gpm
Exhaust air: 1000 cfm
Direct labor: 2 @ $5/hour

8) AR Coating by CVD Belt Furnace

Belt furnace: $150,000
Belt-to-belt transfer: $30,000
Area: 100 sq. ft.
Materials: Nitrogen, Ti $(OC_3H_2)_4$, 2¢ wafer
Utilities: Electricity 10 kW
Cooling water 2gpm
Dry air 200 cfm
Direct labor: 1 @ $5/hour

TABLE 13. REQUIREMENTS FOR EACH PROCESS STEP (concluded)

9) Solder dip, clean, test and sort, encapsulate

Equipment: $664,000 (expanded SPI-LINE 1000M)
Area: 620 $ft.^2$
Mtls: per wafer; glass, EVA ribbon, solder, $0.504
Utilities: 43 kW
19 gpm
Direct labor: 11 at $5/hour
1 at $7.50/hour

Table 14 shows that the more costly process (per wafer) of furnace annealing with a surface passivating oxide is the most cost effective of the ion-implantation and annealing process sequences studied based upon dollars/watt pricing. This is due to the high efficiency achieved.

The lowest cost per wafer in the diffused junction cell process is due to the higher fraction of uptime in this line (85% versus 80% for the ion implanter). The cost of diffusing a junction in one wafer was greater than the cost of ion-implantation and furnace annealing with an oxide layer grown (27¢ versus 25¢) but the greater average uptime lowers the cost of all other processing. The efficiency given for this process is a pessimistic assumption.

TABLE 14. IPEG ANALYSIS SUMMARY (for 3MW/yr line)

Process	$/Wafer	Efficiency	$/Watt
(a) Laser Anneal	6.45	12.6	6.56
(b) Furnace Anneal with oxide	6.39	14.1	5.81
(c) Furnace Anneal w/o oxide	6.35	12.7	6.41
(d) Spray-on diffusion	6.29	13.0	6.20

* Efficiency in percent at AM1 illumination, 100 mW/cm^2. with screen printed contacts, 78 cm^2 area.

SECTION 6
CONCLUSIONS

The results of this program indicate that pulsed excimer laser annealing of ion-implanted junctions in crystalline silicon wafers with screen printed contacts and AR coating is not cost effective compared to furnace annealing with the growth of a surface passivating oxide, which results in more efficient solar cells at lower cost per watt. The recent completion of a 9MW/yr crystalline silicon solar cell factory using ion-implantation and furnace annealing for doping, with its product selling competitively to the output of diffused cell factories, attests to the viability of this approach.

REFERENCES

1. R.F. Wood, et al in Pulsed Laser Processing of Semiconductors v.23 of Semiconductors and Semimetals (Academic Press, New York, 1984) Chapter 10.

2. E.T. Shtyrkov et al, Sov. Phys. Semicond. 9, 1309 (1976).

3. A.R. Kirkpatrick, U.S. Patent 3,950, 187.

4. M. Oron and G. Sorenson, Appl. Phys. Lett. 35, 782 (1979).

5. R.T. Young et al Appl. Phys. Lett. 43, 666 (1983).

6. Questek, Billerica, Massachusetts.

7. G.A. Landis et al, Rec. of 15th IEEE Photovoltaic Specialists Conf. (1981).

8. R.T. Young et al, Mat. Res. Soc. Symp. Proc. 13, 410 (1983).

9. J.S. Katzeff et al, Proc. 3rd E.C. Photovoltaic Solar Energy Conf., 708 (1980).

10. R.T. Young, Mat. Res. Soc. Symp. Proc. 23, 217 (1984).

11. C.W. White et al, Pulsed Laser Processing of Semiconductors, op. cit. Chapter 5.

12. P. Ostoja et al, J. Appl. Phys. 52, 6208 (1981).

13. A. Greenwald et al, J. Appl. Phys. 50, 783 (1979).

14. R.W. Aster and R.G. Chamberlain, Jet Propulsion Laboratory technical report 5101-33 (1977).

15. P. J. Fimett, J.P.L. Tech. Report 5101-60, Rev. A (1979).

16. M. Spitzer and C. Keavney, "Processing Technology for High Efficiency Solar Cells", Presented at the JPL Research Forum on High Efficiency Solar Cells, 1984.

Quotes for Questek

March 1985

50 Watt KrF Laser Annual Operating Budget Estimate
(1 shift operation, 5 days/week, 52 weeks)

Initial Purchase	Total cost
Laser (330 mJ/pulse @ 150 Hz)	48,000
Cryogenic Gas Processor	6,500
Spare Parts	
Thyratron	5,000
Capacitors	1,000
Optics	1,500
Misc. Elect.	2,000
	64,000

Annual replacement Parts

Item	Est. Life(hrs)	Units /Year	Unit Cost	
Thyratron	2,800	0.75	5,000	3,750
Capacitors	1,400	1.5	1,000	1,500
Electrodes	4,000	0.5	1,500	750
Preionizers	1,400	1.5	600	900
Optics	400	5	1,500	7,500
H.V. Power Supply	4,000	0.5	1,500	750
Main Laser Chamber	8,000	0.25	5,000	1,250
				16,400

Gas Cost @ 3 fills/day, Ne-based

Krypton @ 16/fill	12,480
F2 @ .68/fill	530
Ne @ 25/fill	19,500
	32,510

Gas Cost @ 4 fills/day, He-based

Krypton @ 16/fill	16,640
F2 @ .68/fill	700
He @ 2/fill	2,080
	19,420

Liquid Nitrogen Cost @ 1 fill/day (10 liters/fill @ 0.38¢/liter)	988

QUESTEK INC., 7 DE ANGELO DRIVE, BEDFORD, MA 01730 (617) 275-3450

	Total Cost
Power @ 11¢/kWH (3.6 kW supply)	824
Maintenance @ 25/hr	
Standard (0.5 hr/day)	3,250
Periodic (1 hr/week)	1,300
	5,374
Service* @ 75/hr	
3.25 hrs/mo	2,925
	122,197**
TOTAL	109,107***

* Service Time Breakdown

Item	Service Time (hrs)	Units/Yr
Thyratron	4	0.75
Storage Caps.	4	1.5
Electrodes	8	0.5
Preionizers	8	1.5
Optics	2	5
H.V. Power Supply	4	0.5
Main Laser Chamber	8	0.25

** Total assuming Ne-based gas mix

*** Total assuming He-based gas mix

APPENDIX A

QUESTECK
SERIES 2000 EXCIMER LASERS

questek

Series 2000 excimer lasers

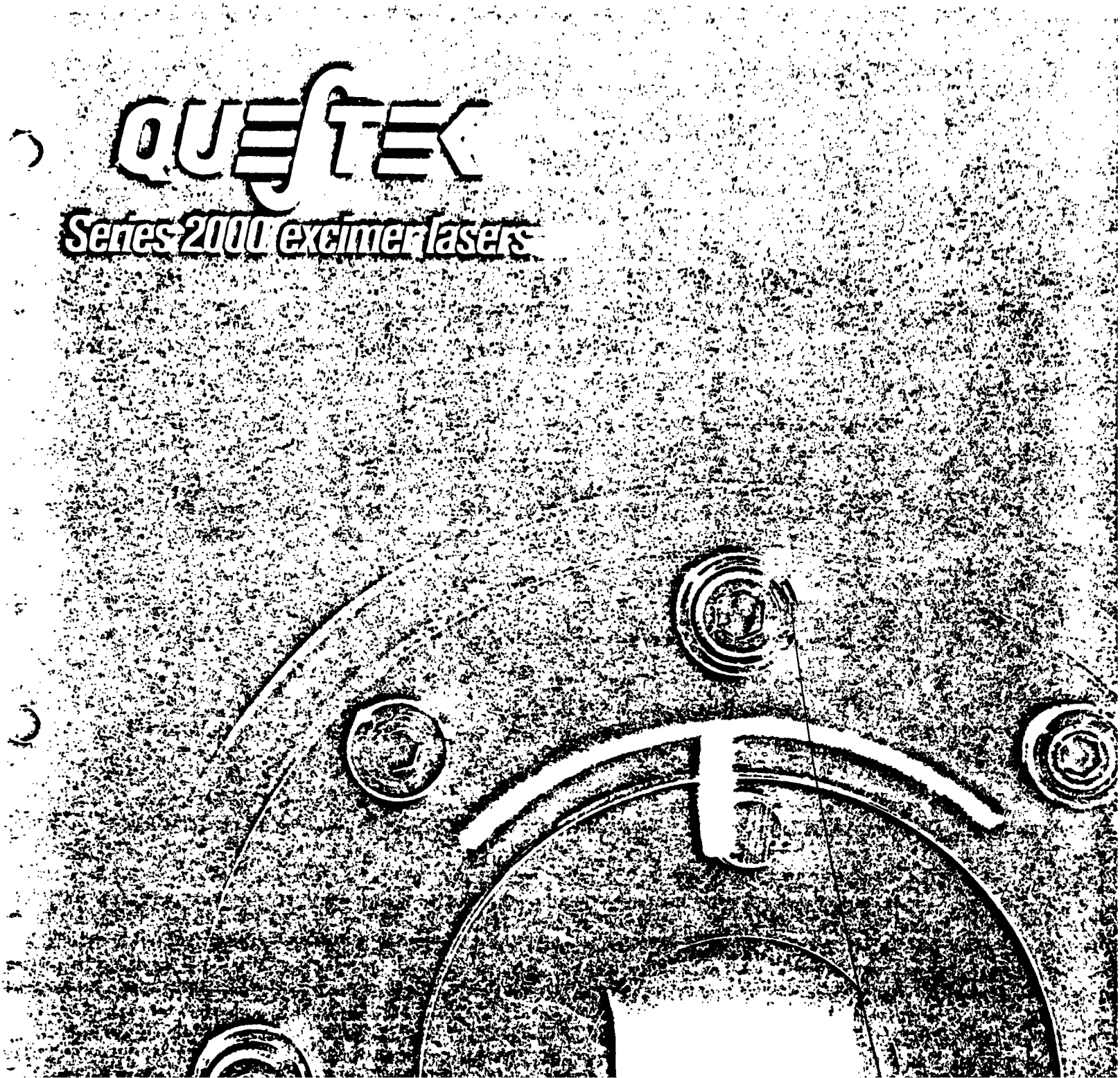

Characteristics of Excimer Lasers

Excimer lasers are unique light sources which provide high power ultraviolet pulses at any one of a number of fixed wavelengths. The output beam of commercial excimer lasers is rectangular with fairly large divergence when standard optics are used. Low divergence beams can be produced with "unstable resonator" optics, but with a sacrifice in energy. The excitation is normally produced by a high speed electric discharge, although some large excimer lasers are excited by electron beams.

The fuel gas mixture contains a small concentration of a halogen (chlorine or fluorine) and rare gas (argon, krypton or xenon) in a buffer of helium or neon. Upon excitation the halogen and rare gas atoms combine to form a rare gas halide molecule which emits at a discrete wavelength in the ultraviolet in the range from 193 to 351 nm.

Rare gas halides which exhibit the most intense output are ArF (193 nm), KrF (248 nm), XeCl (308 nm) and XeF (351 nm); single-pulse energies from these species are typically between 0.1 and 1.0 Joule. The average power produced by an excimer laser is limited by its pulse repetition frequency (PRF). Most commercial excimer lasers produce a few tens of watts average power.

The scaling of average power with the PRF depends on the capacity of the high voltage power supply and the gas flow and cooling systems. In efficient flow designs which replace the gas between electrodes several times between pulses, the pulse energy remains constant and the average power scales linearly with the PRF. Due to flow limitations, most excimer lasers operate at a maximum PRF of a few hundred pulses per second.

The maximum output of all excimer lasers degrades with time as the halogen is consumed and reaction products absorb and scatter at the laser wavelength. A feedback control circuit must be used to operate the laser at a constant level below the maximum available power. Useful gas-fill lifetimes typically vary from a few hundred thousand pulses to more than ten million. Lifetimes vary with the operating wavelength selected and depend on a number of factors, including pulse energy, gas purity, discharge circuit design, construction materials, contaminant removal rates and cleanliness of the cavity optics. Lifetimes at constant power also depend on the amount of "reserve power available"—the difference between the operating power and the maximum power available from the laser.

The unique combination of high peak power ultraviolet pulses at high average powers makes excimer lasers suitable for a wide variety of applications, including photochemistry, dye laser pumping, materials processing, medicine, remote sensing and Raman shifting.

Table of Contents

System Design	4
Pulsed power system	6
Microprocessor controller	8
Powerlok	12
Boost	13
Beam characteristics	14
Optional accessories	16
Choosing the model	18
Specifications	19
Questek background	20

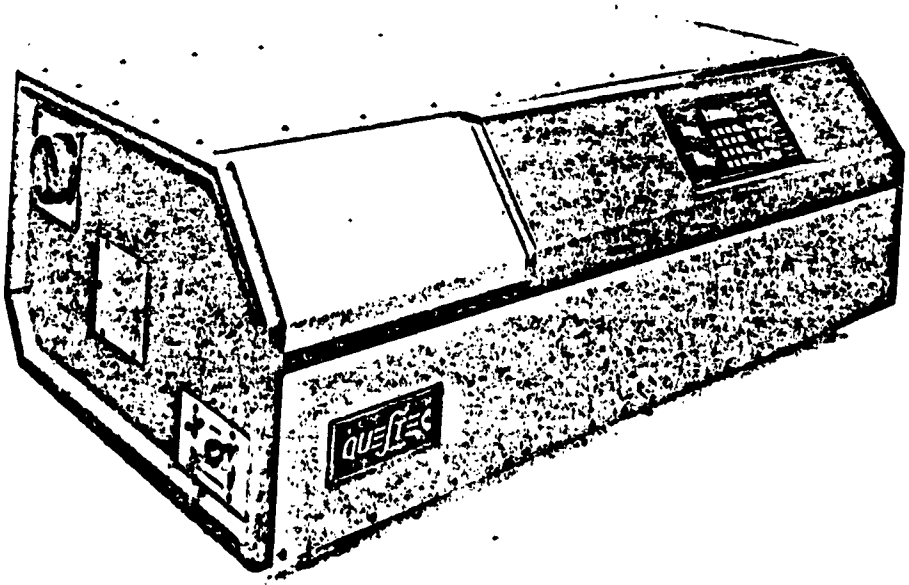

Questek Series 2000 Excimer Laser

Questek offers a broad product line of excimer lasers ranging in pulse energy from 40 mJ to 750 mJ and in repetition rate from 20 Hz to 400 Hz. Each model is based on Questek's unique high-efficiency design. Each laser includes a built-in microprocessor to control the laser output power, gas filling and system diagnostics. The performance and features available in the Series 2000 lasers are unmatched by any other commercial laser.

The following pages describe the Series 2000 lasers, from broad design goals to details of the circuit and output beam characteristics. The specifications for the five energy classes are shown at the rear. While attempting to be comprehensive, we cannot cover every aspect of the Series 2000 lasers. We invite questions on our toll-free number in the U.S.: 1-800-EXCIMER. Customers outside the U.S. and Canada should contact the local Questek distributor.

A Variety of Applications

Photochemistry
- excitation and fragmentation studies
- thin-film deposition
- ablation of polymers
- laser enhanced industrial process syntheses

Dye Laser Pumping (1)

Materials Processing
- semiconductor annealing
- photolithography
- microcircuit repair
- chemical vapor deposition
- microetching
- precision drilling
- product marking

Medicine
- refractive surgery (vision correction)
- plaque removal (laser angioplasty)
- microsurgery

Nonlinear processes
- multiphoton excitation/ionization
- laser triggered switches

Remote sensing

Raman shifting

1. Questek excimer lasers will pump any of the commercially-available dye lasers without compromising performance. Consult Questek for details.

Series 2000-processed microcircuit showing selective removal of polymer overcoat to expose conductive element without damage to circuit structures. Magnification is 2000×. Photo courtesy of Sperry Corp.

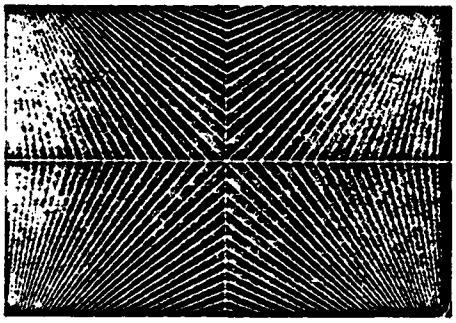

Photovoltaic cell annealed by Series 2000 laser and ready for incorporation into a solar cell array. Pulsed excimer laser annealing (PELA) of ion implanted junctions provides a cost-effective replacement for diffused junctions in silicon solar cell fabrication. Photo courtesy of Spire Corp.

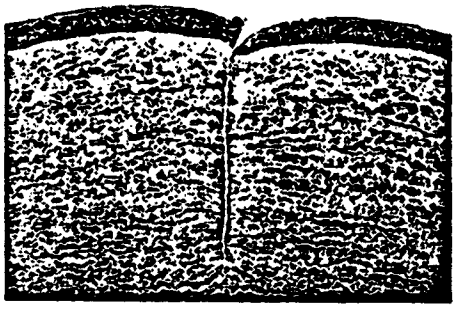

Experimental incision in the cornea made using a Series 2000 excimer laser. The incision is approximately 20 μm wide and hundreds of micrometers deep. The notable absence of tissue alteration adjacent to the incision is not possible with conventional laser therapeutic tools. Magnification is 33×. Photo courtesy of Dr. Carmen A. Puliafito, Massachusetts Eye and Ear Infirmary.

Cross-section of myocardium showing sites of excimer laser tissue removal. Note the absence of thermal charring in tissues adjacent to the laser incisions. Excimer lasers have also been used to achieve selective removal of atherosclerotic plaque. Photo courtesy of Dr. Jeffrey M. Isner, Tufts University New England Medical Center.

Series 2000 System Design

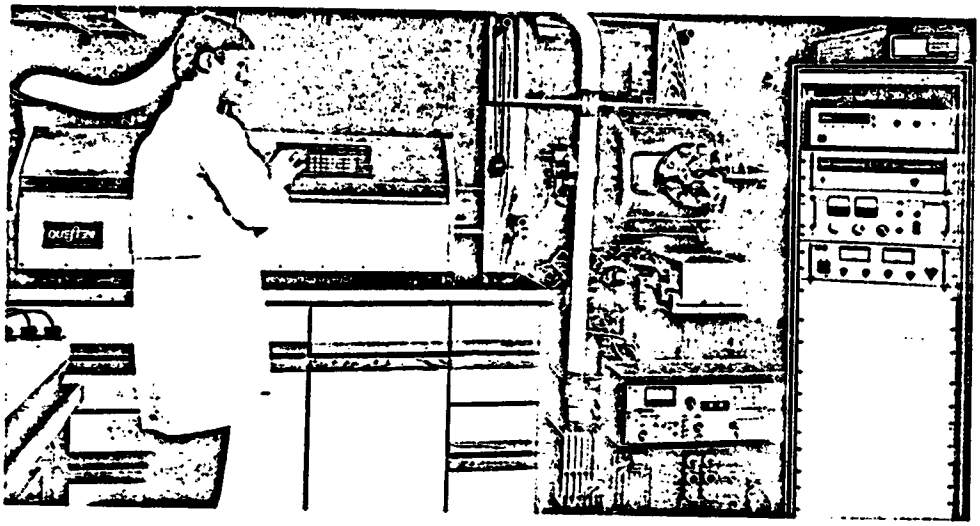

Design Requirements

Before designing the Series 2000 Excimer Lasers, we asked several users of similar lasers what they wanted. After all, we were not encumbered by previous designs —instead we had a "clean sheet of paper." This is what we heard.

Constant Power

One of the most irritating characteristics of previous excimer laser designs is the decline in output power with time. In extreme cases, the specified power is maintained for only a few minutes. Users now require constant power control as a standard feature.

Reliability

Most problems with pulsed gas lasers occur in the high voltage pulsed power system; thus this system must receive the greatest attention. The circuit must be carefully designed to produce minimum component loading, even if output energy is sacrificed. The pulsed power system must be designed as an integral unit, not assembled from separate subsystems. Components must be operated well below rated specifications, including energy storage capacitors and the high voltage power supply.

High Efficiency

High efficiency means that the laser maximizes output relative to the energy stored on the primary capacitors. Thus a specified level of performance is achieved with minimum loading on the system. The consequences of this approach are significant, because

- Electrical stress on components is minimized
- EMI is reduced
- Gas lifetimes are increased
- Electrode erosion rates are reduced

Versatility

To be an efficient tool of general utility, an excimer laser needs to operate under a variety of conditions and with different gas mixtures. The laser design should permit field upgrades to extend the performance range of the original instrument and offer a number of operating modes, including provisions for triggering from an internal or external source, use of command charge, and a wide selection of energy ranges. Low-divergence optics should be available for more stringent applications.

Ease of Use

As new excimer laser applications continue to develop, ease-of-use becomes increasingly important as a design criterion. Earlier generations of excimer lasers were state-of-the-art instruments for which performance, not ease-of-use, was the main design objective. A new excimer laser must emphasize ease-of-use without sacrificing performance.

Ease of Service

With the development of industrial and medical applications for excimer lasers, ease of service becomes increasingly important. Lasers should be equipped with sufficient test points and status indicators to permit rapid problem isolation; diagnostic aids should be included to monitor performance parameters without interfering with operation; subassemblies should be readily accessible to permit rapid replacement.

Our Solution

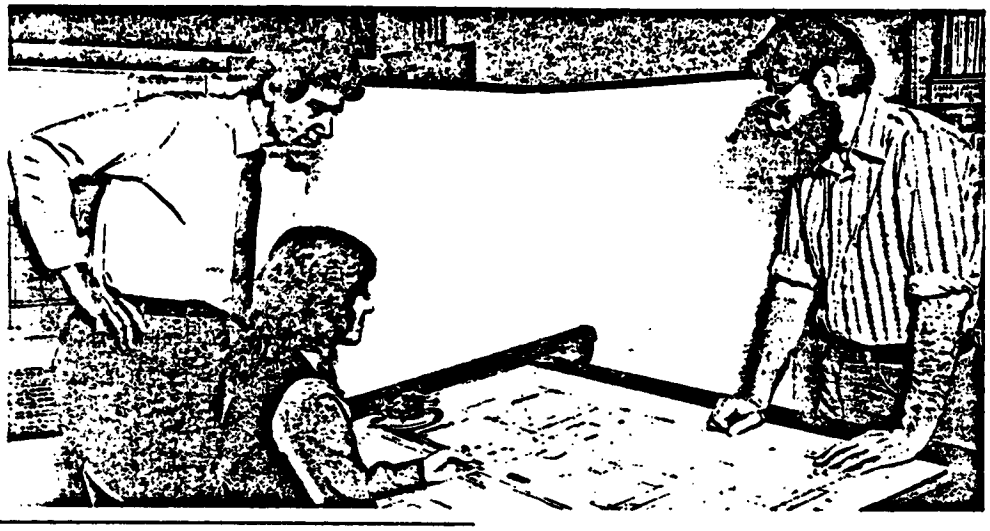

What did we do to satisfy these requirements? We designed the laser as a system from the ground up with each of these items in mind. And we built-in all of the standard features from the start rather than adding them on later.

We installed a microprocessor controller and introduced Powerlok™—a patented technique to maintain constant power. As part of the controller we built in an energy and power meter with digital display of the laser output.

We brought to bear years of experience in high voltage power supplies, capacitors and thyratron switches to design the pulsed power system. We appreciated the limitations of existing circuits that produced undesirable "aftercurrent," and designed a circuit with minimum aftercurrent and no reverse current. (See Technical Note #1.) The circuit is the simple "capacitor discharge" design which avoids complicated and expensive magnetic pulse compression. Next, we selected a long-life thyratron to handle the load, and added "magnetic assist" to reduce tube dissipation. Finally, we insured that all the components were conservatively rated and had long records of reliability in other similar applications.

The discharge circuit configuration for Series 2000 lasers achieves an optimum balance between primary and secondary capacitance which generates minimal aftercurrent yet maximizes efficiency. Secondary capacitors are located inside the discharge chamber to reduce inductance, and the energy loading in the gas is chosen to optimize pulse energy. The resulting efficiencies are the highest in the industry:

ArF	*2.0%*	*XeCl*	*2.5%*
KrF	*3.5%*	*XeF*	*2.0%*

We used passive materials in the construction of the discharge chamber of the Series 2000 lasers to permit rapid conversion between chlorine and fluorine-based mixtures without lengthy re-passivation. Our lasers are true multigas systems and need not be dedicated only to chlorides or only to fluorides.

Each laser can be operated with reduced energy at twice the normal repetition rate. We employed modular construction of the power supply, storage capacitor and electrode assembly to facilitate field upgrades. Optional unstable resonator optics provide low-divergence performance.

We made one of the most significant advances in commercial excimer laser designs by incorporating a microprocessor controller as standard in all Series 2000 lasers. While designed to maintain constant power, the controller makes these lasers incredibly easy to operate. The user selects the energy and repetition rate, then the controller takes over to run at the prescribed conditions or to stop and refill the laser—all automatically. Thanks to Questek, gone are the days of watching pressure gauges or turning valves manually.

We designed a diagnostic system to monitor key operating parameters in the laser. If the system senses a fault condition, it turns off the laser and displays an appropriate error message. This is the first line of protection to minimize potential damage—particularly to the high voltage system. Once a fault has been detected, diagnostic test points can be used to quickly locate the cause.

Totally Integrated Pulsed Power

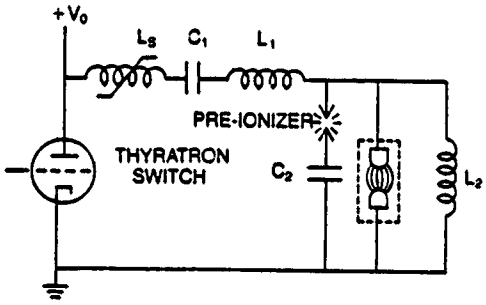

Capacitor discharge circuit design. When the thyratron is triggered, energy stored in C_1 is transferred to C_2 and subsequently discharged into the excimer gas load. L_S represents a saturable reactor which delays the current pulse ("magnetic assist"). The gap between L_1 and C_3 represents the provision for preionization.

As the most important part of the laser, the pulsed power system was designed as an integrated unit. Questek's understanding of high-voltage technology and the details of excimer laser circuit dynamics is evident in the design.

Capacitor Discharge Circuit

The Series 2000 lasers use the "capacitor discharge" circuit shown in the figure. This is the most straightforward circuit for a discharge-pumped excimer laser, and is the most common. However, if the circuit parameters are not chosen carefully, severe aftercurrent results—dramatically decreasing component lifetime. (See Technical Note #1.)

Questek has tailored the discharge circuit to provide minimum aftercurrent and no reverse current. The components chosen have years of field-proven experience in pulsed gas lasers. This simple and carefully designed circuit is a major step toward high reliability in the pulsed power system.

It is the strength of this circuit that allows Questek to back the entire pulsed power system with a two-year warranty—the strongest in the industry.

Thyratron

Because the Series 2000 discharge circuit generates minimal aftercurrent, a conventional, grounded-cathode thyratron can switch the stored energy. The tube always operates in the "glow" mode, and its lifetime is extended significantly not only by reduced loading, but also by the use of magnetic switching. The relatively low operating voltage of 20–30 kV permits the use of an inexpensive single-stage tube rather than the double-stage tubes required at higher voltages.

Magnetic Switching

Questek uses a magnetic switching technique called "magnetic assist" to prolong thyratron lifetime by reducing tube dissipation. (See Technical Note #2.) The saturable inductor next to the thyratron delays the current for 10–15ns, allowing the tube voltage to drop as the plasma expands before high currents develop.

The Series 2000 lasers do not use magnetic pulse compression because this technique is necessary only in higher power lasers. Magnetic pulse compression does reduce the peak thyratron current, but this is not a factor in low and medium power lasers. Technical Note #4 compares the capacitor discharge circuit of the Series 2000 lasers with a commercial circuit using magnetic pulse compression and shows that the thyratron loading (RMS current) is the same for lasers with equal efficiencies. Thus the added cost and complexity of pulse compression is not justified until the thyratron current is at its rated limit, and this does not occur until average power levels reach approximately 100 watts.

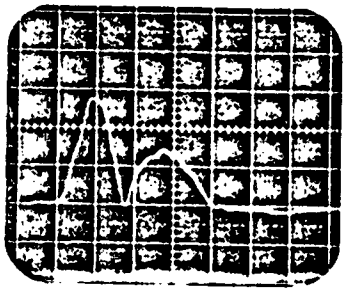

Thyratron current waveform for Series 2000 demonstrating minimal aftercurrent.

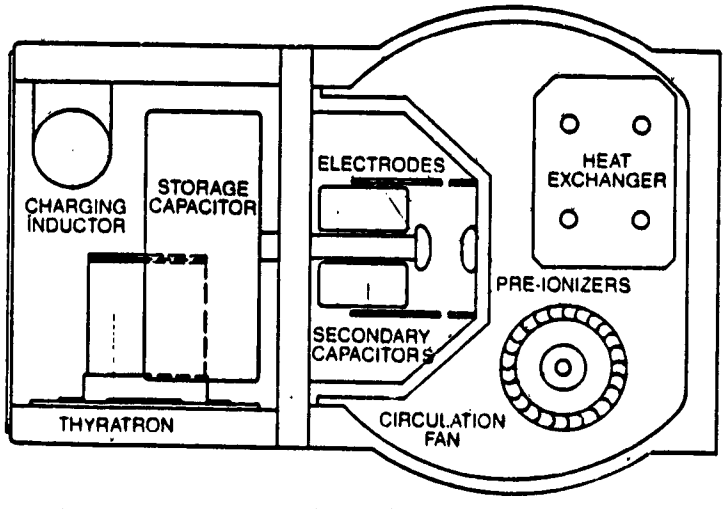

Cross-section of laser chamber and discharge circuit.

High Voltage Power Supply

Questek designed a family of highly-regulated switched-mode power supplies specifically for the Series 2000 lasers. These supplies are compact in size and differ only in average power capacity. Each unit is mounted inside the laser adjacent to the storage capacitor load. As a result, electromagnetic interference (EMI) is totally contained and failure-prone coaxial high voltage cables are eliminated.

In operation, the power supply charges the storage capacitors to a regulated voltage controlled by the microprocessor. In the internal trigger mode, the supply only operates "on command" and charges the capacitor just before a laser pulse to minimize time at high voltage. In the external trigger mode, this command charge mode may be ON or OFF; when it is OFF, the capacitors are fully charged at all times between laser pulses and will remain so without "pre-firing" at any repetition rate. This mode is used when the laser emission must appear promptly (1 microsecond delay) relative to the trigger pulse and with minimal temporal jitter (see page 15).

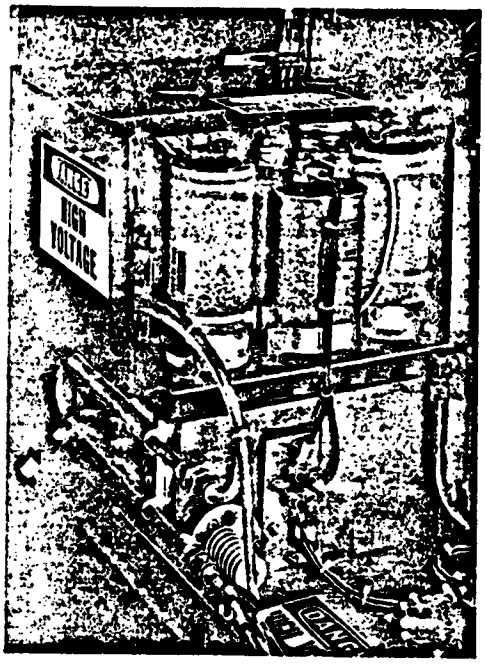

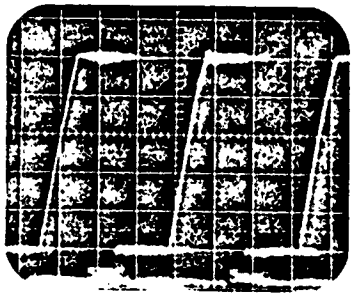

Voltage waveform produced by the HVPS. Scale is 5 kV/div. Command charge mode is ON.

Compact, switched-mode high voltage power supply (HVPS) is located inside the laser for minimal EMI.

Discharge Chamber

The discharge chamber is made of nickel-plated aluminum for strength and halogen resistance and encloses the electrode assembly, gas circulation fan and heat exchanger. The end plates of the chamber support the cavity optics, the filtered-gas return system from the gas processor (which "washes" the optics; see page 9), and the circulation fan drive shaft. All metallic surfaces exposed to the halogen gas mixture are either solid nickel (those in close proximity to the main discharge) or nickel plated.

The heat exchanger is a "tube and fin" design. All seals are outside the discharge chamber, thus eliminating the possibility of a water leak inside the chamber. The base metal of the heat exchanger is copper which has superior resistance to corrosion by water.

Electrode Assembly

Questek has designed modular electrode assemblies so the user can easily extend the performance range of any laser through rapid and cost-effective model upgrades. The electrode assemblies are the key to the high discharge efficiencies achieved by Series 2000 lasers. Each assembly consists of the main electrodes, preionizer and secondary capacitor arrays mounted to a chemically inert dielectric slab. The assembly is easily inserted into the discharge chamber and is readily accessible for service.

The spark preionizers function as a quasi-line source of ultraviolet light adjacent to the discharge for efficient and uniform preionization. The secondary capacitors are placed inside the chamber for high efficiency and are hermetically sealed with chemically inert coatings to insure long gas lifetimes. Metallic parts are either solid nickel or nickel-plated for maximum halogen resistance.

The electrodes are solid nickel and last significantly longer than designs utilizing nickel plating or cladding over other base metals. The overall design of the assembly permits efficient heat removal from the electrodes—even under high average power conditions. Erosion rates for the main electrodes are extraordinarily low—so much so that Questek guarantees the electrodes for the life of the product.

Modular electrode assembly is easily accessible and interchangeable in the field with alternate configurations.

Our Standards Are Other's Options

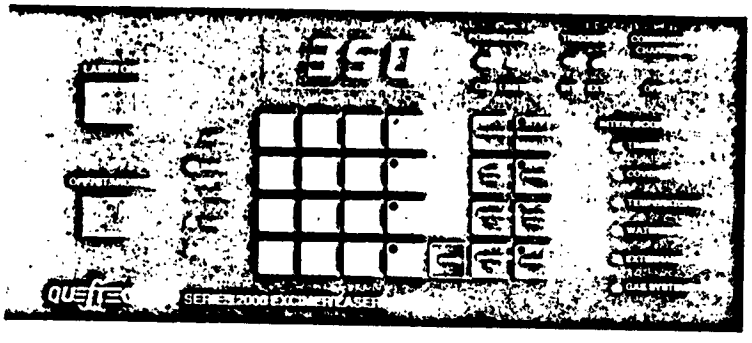

The Series 2000 control panel showing keypad, digital display, and status indicator lights.

Microprocessor Controller

Microprocessor control is standard in every Series 2000 laser. This Questek innovation puts the Series 2000 lasers in a class by themselves—distinct from other lasers which may add a microprocessor as an accessory. The integrated Questek design has been in every Series 2000 laser since 1983 and is unsurpassed in its performance and in its multitude of functions.

- *Powerlok*—Maintains constant output energy by controlling the gain of the laser medium, either by changing the high voltage or gas mixture or both.
- *Automatic gas control*—Refills the laser automatically and controls BOOST.
- *Repetition rate*—Generates an internal repetition rate of exceptional accuracy.
- *System parameters*—Stores user-defined parameters in a non-volatile memory. Prevents the selection of unsafe operating conditions.
- *Diagnostics system*—Monitors system performance and warns the user of unusual conditions; disables the laser if a dangerous condition develops.

If necessary, the microprocessor can be bypassed and the laser run in a "manual" mode with an external pulse generator.

Control Panel

All laser functions can be controlled and monitored from the control panel located conveniently on the front of the laser chassis. The clearly labeled keypad enables the operator to choose the parameter to monitor or alter—whether it be pulse energy, average power or pulse repetition rate.

Single key-stroke command sequences control system evacuation, chamber purge and automatic gas filling. In addition, the versatility of manual gas fill control is provided with individual halogen, rare gas and buffer gas switches. The various laser operating modes—such as Powerlok, trigger source and command charge—are all individually selected and their status displayed on the panel. Gas mixture recipes and a variety of operating and performance parameters can be examined or altered via a CODE key. Error code diagnostic messages appear on the display as appropriate. The BOOST function provides for the automatic replacement of gases during laser operation to prolong continuous operating time (see p. 13).

Pulse Energy/Power Monitor

Every Series 2000 laser incorporates a pulse energy/power monitor which enables the output to be measured while the laser is being used.

A beamsplitter collects a small fraction of the output beam to be measured. A diffuser and collecting cone insure that the pyroelectric detector samples the entire beam to give a measurement of the output energy accurate to ± 5% for all gases. A calibrated analog signal for individual pulse energies is supplied to the I/O panel for external monitoring. Energies from successive pulses are averaged by the microprocessor and displayed as either pulse energy or average power. This pulse energy monitor is used as the "first line" diagnostic and safety feature—if the energy drops below the expected value for any reason, the laser is turned off and an error message displayed.

Pulse energy monitor configuration.

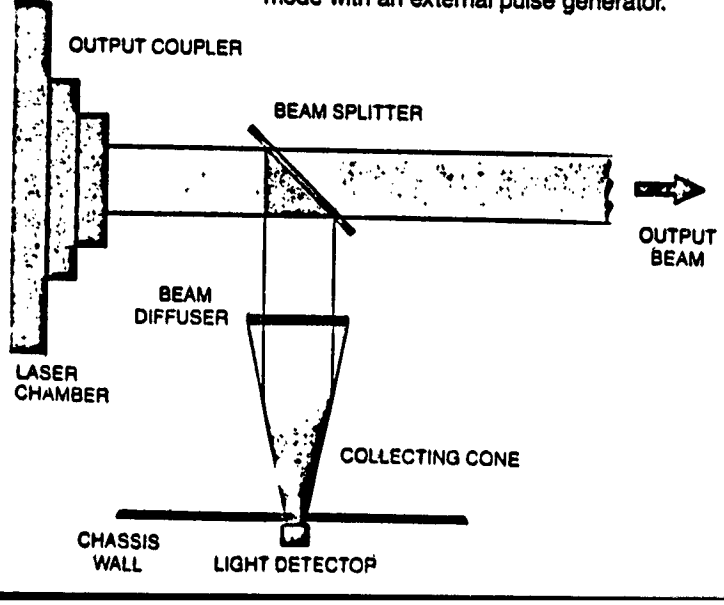

Chassis Construction

In order to create an effective barrier to the electrical noise created by the laser, the chassis is made of heavy-gauge nickel-plated steel. The superiority of steel—as opposed to other metals—in the suppression of EMI made it the logical choice as the chassis construction material. (See Technical Note #5.)

Except for the top covers, the chassis is a single unit with seam welds at each edge to insure continuity. The nickel plating provides a durable surface of high conductivity and is ideal for the large-area EMI gasketing between the covers and the main chassis.

Apart from the output beam port, each chassis opening is electrically and magnetically shielded. As a result, the magnitude of the radiated noise is a factor of five to ten below other lasers.* It is this excellent shielding that allows the microprocessor controller to function reliably in the electronics compartment rather than in a remote console.

Consult Questek for details.

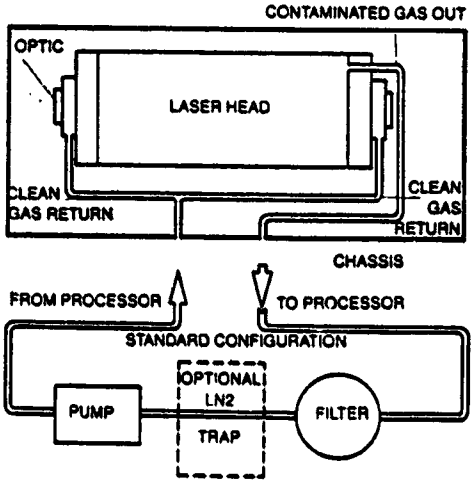

Questek gas processor configuration, showing particulate filter and circulation loop.

Electronics Compartment

A completely self-contained electrically-shielded compartment is provided within the laser chassis to protect all sensitive components from the EMI of the discharge. It contains the microprocessor and display circuit boards, signal I/O panel, low-voltage power supply, pulse energy monitor, and a non-resettable mechanical pulse counter which records the number of laser pulses in units of 1000. There is also a "driver" circuit board which governs the gas system solenoids, circuits for the high voltage power supply, and low voltage trigger circuits. This board has an extensive array of status indicator lights as well as the mode selection switches for Powerlok, trigger source and command charge.

The I/O panel is equipped with MS connectors for remote interlocks and laser remote ON/OFF control. (Mating connectors are supplied with the laser.) BNC connectors are available for external trigger input and pulse energy, high voltage, and chamber pressure signal outputs. The graph on page 12 used standard signals available on this panel.

Gas Processor

Contaminants are produced in all excimer lasers in both gaseous and solid forms (particulates or "dust"). They degrade laser performance by increasing cavity losses, either via absorption or scattering in the cavity. Gaseous contaminants require chemical or cryogenic removal, but particulates can be removed mechanically by simple filtration.

A gas processor which removes particles down to 0.05 microns is a standard feature in each Series 2000 laser. The processor injects clean gas over the optics to prevent deposits from forming on the mirror surfaces. This technique is essential to prolong the interval between optics cleaning, but it does not increase gas lifetimes for KrF and ArF for which gaseous contaminants are the dominant cause of losses. Optional cryogenic processing is described on page 17.

The low-cost disposable filter in the processor unit requires periodic—but infrequent—replacement. Because the processor is located external to the discharge chamber, the filter can be changed without opening the chamber, and replacement requires less than one-half hour.

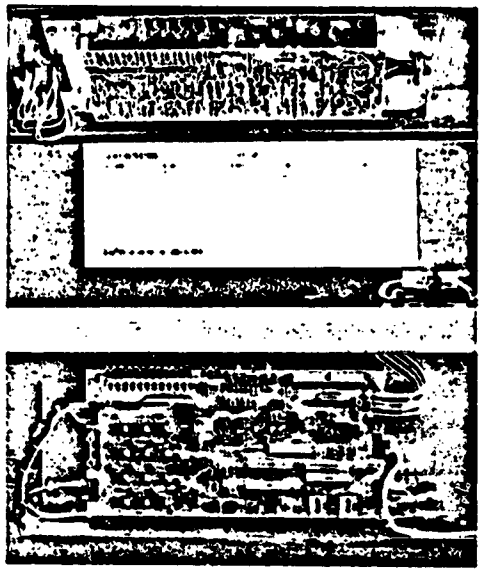

Electronics compartment showing driver circuit board, and microprocessor circuit board. Covers are removed for clarity.

The Series 2000 Excimer Laser

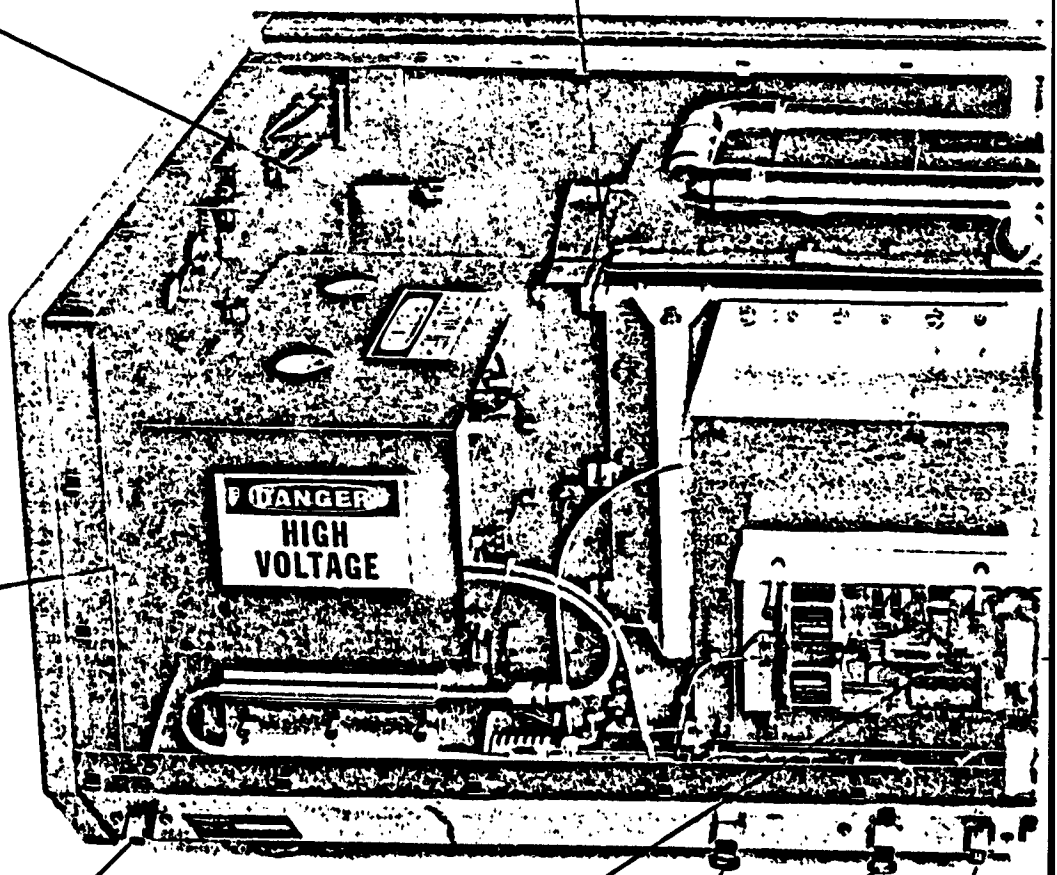

MAIN GAS RESERVOIR

PULSE ENERGY MONITOR CHAMBER

SWITCHED-MODE HVPS

EXTERNAL OPTICS PURGE

THYRATRON TRIGGER BOARD

VACUUM PUMP CONNECTIONS

GAS PROCESSOR CONNECTIONS

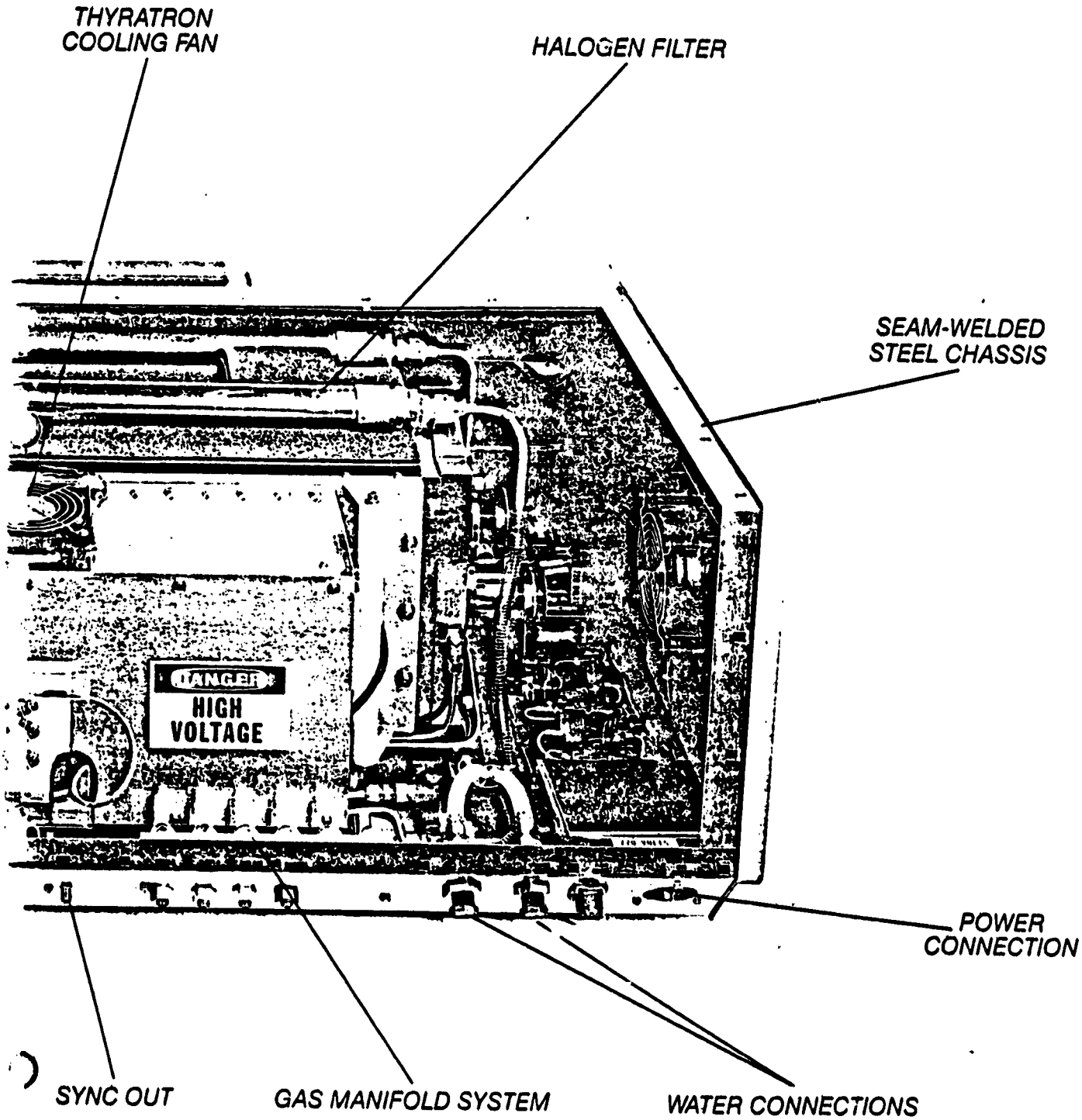
THYRATRON
COOLING FAN
HALOGEN FILTER
SEAM-WELDED
STEEL CHASSIS
DANGER
HIGH
VOLTAGE
POWER
CONNECTION
SYNC OUT
GAS MANIFOLD SYSTEM
WATER CONNECTIONS

The Constant Power Solution

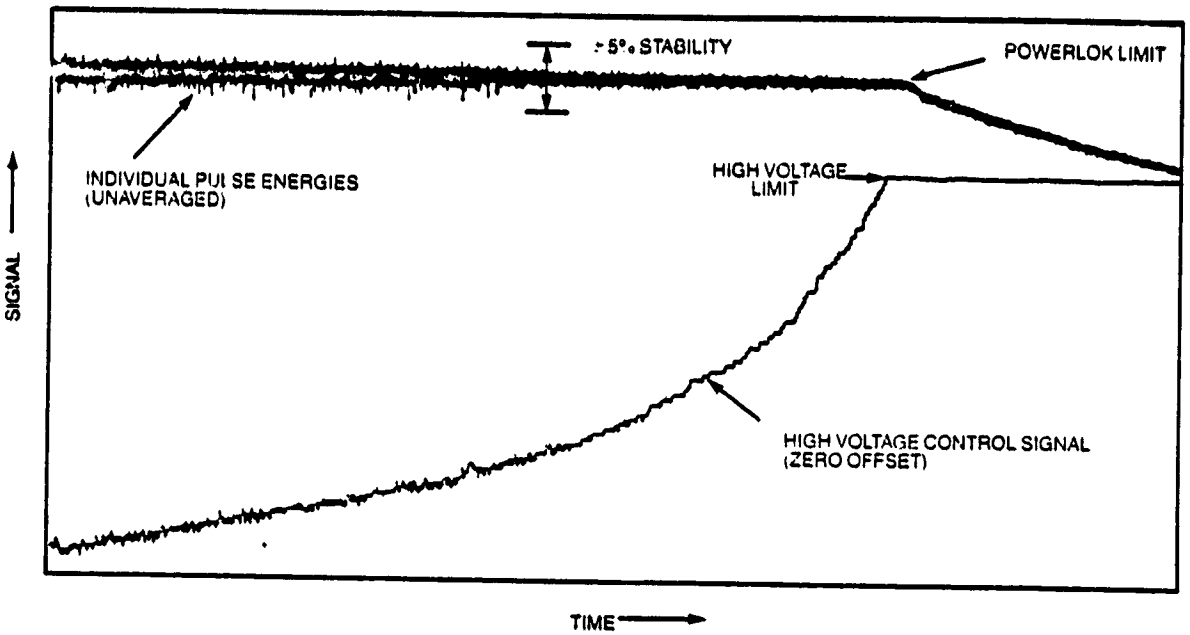

Pulse energy and Powerlok control voltage as a function of time for a single KrF gas fill. Top curve shows individual (unaveraged) pulse energies. Note the decrease in output after the Powerlok limit is reached. Bottom curve shows individual control voltage steps on an expanded, offset scale for clarity. Maximum voltage corresponds to Powerlok limit.

Powerlok

Under fixed operating conditions, the pulse energy of all excimer lasers gradually declines as the halogen is depleted and the gas mixture becomes increasingly contaminated. Questek was the first excimer laser manufacturer to address this performance constraint by developing Powerlok —a standard feature in all Series 2000 lasers—which provides constant pulse energy and average power. Powerlok functions by first sampling the output beam using a high-speed detector and comparing a running average of the output with the desired pulse energy level selected at the control panel. Microprocessor circuitry uses any resultant error signal to control the gain of the laser by changing the high voltage or the gas mixture to maintain constant energy.

Powerlok without gas replenishment

In this mode only the high voltage is used to control the gain of the laser. As the gain decreases, the high voltage gradually increases to maintain constant energy as the graph below indicates. When the reserve gain is depleted (maximum high voltage is reached) the output energy declines. Thus the Powerlok energy maximum is limited to that energy achieved at maximum voltage. The Powerlok energy minimum is limited to approximately 50% of the maximum and corresponds to a region of instability near laser threshhold. In order to reduce the energy further, the gas mixture must be modified.

Optimum Powerlok performance is obtained between these limits at 60–75% of the maximum output. The laser efficiency peaks in this range and there is sufficient reserve gain to insure long-term performance before reaching the high voltage limit. The total operating time under Powerlok without gas replenishment depends on many factors including the amount of reserve gain, pulse energy, gas purity, repetition rate, and the general condition of the system. Firm numbers for any wavelength can be defined only in specific operating conditions.

As an example, consider XeCl, a gas which does not require cryogenic processing and for which gas replacement during operation is expensive. For a Model 2240 operating at 150 mJ (75% of specified output) and 100 Hz, the time at constant power exceeds 40 hours.

BOOST

Controlling the high voltage is only one way to maintain constant power in an excimer laser—replenishing the gas mixture is another. Questek invented the concept of gas replenishment for excimer lasers and was the first manufacturer to implement it commercially with the feature designated as "BOOST." This feature maintains constant power by economically replacing fractions of partially contaminated fuel gas with fresh constituents during laser operation. The effect of BOOST is to extend continuous laser operating times, and it is particularly beneficial with inexpensive mixtures which are otherwise short-lived, such as ArF. The BOOST function is performed slowly enough that the output energy does not change during operation.

BOOST without high voltage control

There are several operating modes for BOOST, most of which combine gas and high voltage control. There are times, however, when the high voltage must be kept constant. For example, in some critical timing experiments the jitter from an external trigger must be minimized. A change in high voltage will change the delay from trigger to laser pulse. In this case, a constant voltage can be selected in advance; the laser is filled with a mixture lean in rare gas or halogen, and as the gas is consumed, more is added by the microprocessor to keep the output constant. As in high voltage control without BOOST, this mode is ultimately limited by the reserve gain.

BOOST with high voltage control

The best results are usually obtained by combining gas control with high voltage control. Consider a system with optimum gas mixture operating at 75% of maximum energy. From the graph on the opposite page, it is clear that most of the increase in high voltage occurs near the end of the operating period. (Higher voltages create more contaminants which reduce the gain.) This "end effect" can be avoided by adding fresh gas or replacing some of the original gas during operation.

BOOST is activated at a threshhold voltage, defined by the user. Usually, it is halogen depletion rather than contaminants which cause the initial increase in voltage. In Phase I, BOOST injects only a small amount of halogen and measures the resulting decrease in voltage. If a small or no change occurs, BOOST shifts to Phase II; otherwise it periodically injects a small amount of halogen until a target voltage is reached, at which point BOOST stops until the threshhold voltage is reached again. In Phase II, BOOST replaces a user-defined fraction of the original gas over a period of time. As the "old" gas is removed, the voltage increases to compensate for the reduced gain. Then as fresh gas is injected, the voltage decreases to a value below the threshold voltage. If the target voltage has been reached, BOOST returns to its monitoring mode; if not, another partial replacement cycle begins.

In principle, a laser with BOOST active can operate indefinitely under constant power. In practice, running time is limited by many factors, including accumulated errors in the gas mixture. Replacing part of the "old" gas is not as effective in reducing the high voltage as replacing all of the gas. Thus, the rare gas consumption under BOOST is greater than if the laser were stopped and refilled totally with fresh gas. For ArF the rare gas is inexpensive, so BOOST can economically prolong continuous operating time.

Laser output, total pressure and Powerlok control voltage as a function of time for a single gas fill with BOOST operating. Note the small pressure increase when Phase I of BOOST engages as the control voltage passes the threshold point. Subsequent stepwise decrease in pressure corresponds to operation of Phase II of BOOST.

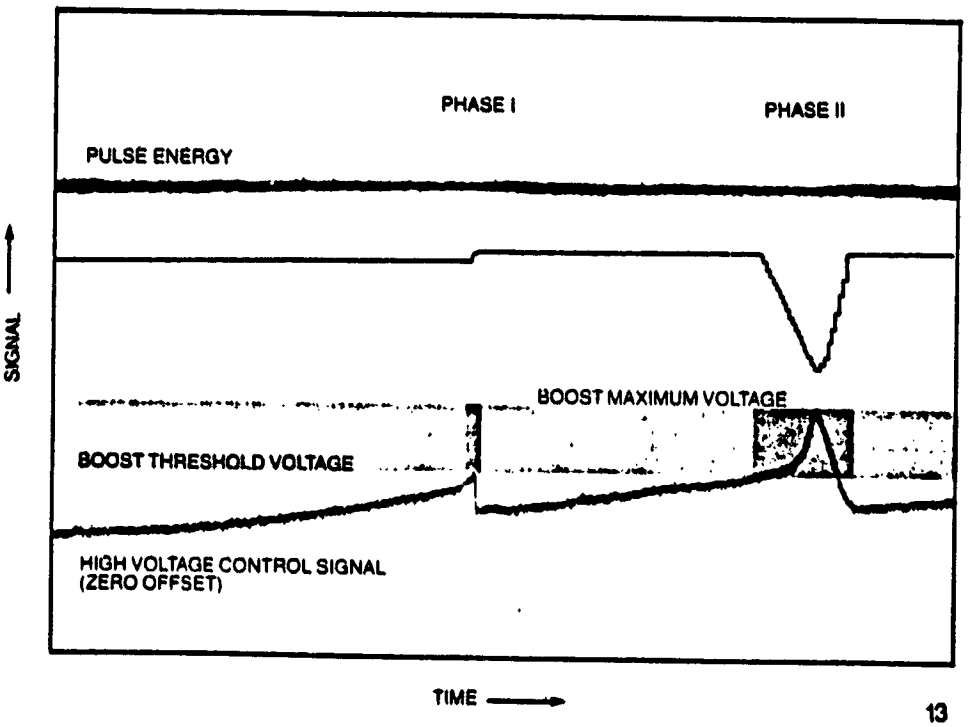

Beam characteristics

2200 MODELS

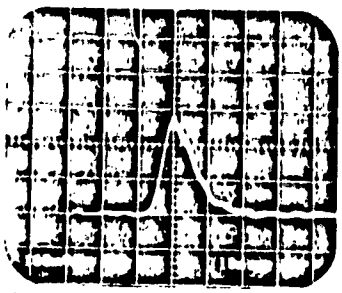

ArF

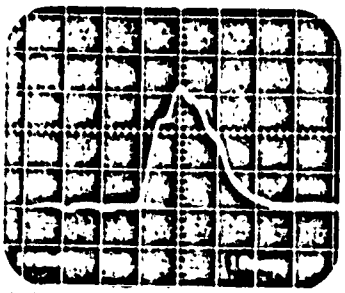

KrF

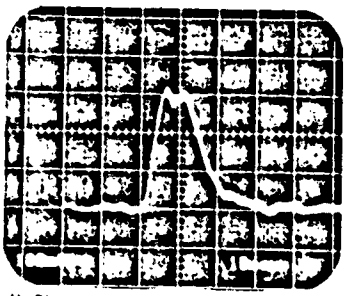

XeCl

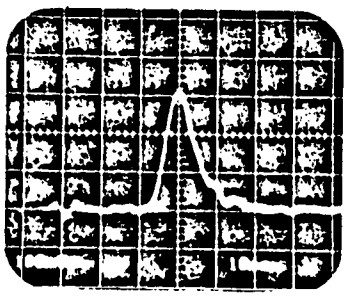

XeF

2600 MODELS

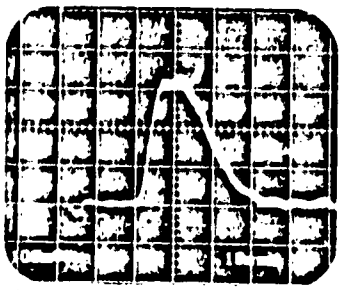

ArF

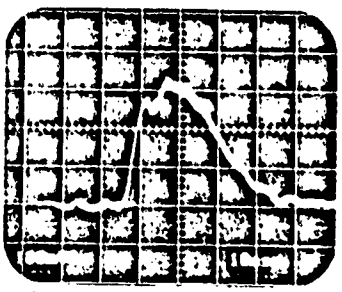

KrF

Temporal Profiles

Temporal profiles for Series 2000 lasers are relatively smooth with little intensity modulation. The full width at half maximum intensity depends on the specific gas mixture and on the pulse energy, and vary from 10ns approximately 25 ns. The pulse width also depends on the operating wavelength, as the accompanying oscillograms show for the 2200 Models. The corresponding oscillograms for the 2600 Models show slightly longer pulses, and the pulse duration for each gas in each model can be determined from these photos.

The temporal profiles can be modified slightly for particular applications. Decreasing the amount of halogen in the mixture reduces the pulse duration; adding neon as a buffer lengthens the pulses. Each of the profiles shown used mixtures with helium as the buffer gas.

Beam profiles

Beam profiles for Series 2000 lasers equipped with standard, stable resonator optics exhibit smooth intensity distributions with ± 10% variation over the central 80% of the beam. Beam patterns are rectangular in form, with a more flat-topped intensity distribution across the horizontal dimension and a near-gaussian distribution across the vertical dimension. The high degree of uniformity is due to carefully optimized electrode profiles and an efficient UV spark preionization geometry.

Scanned array beam profiles for ArF with standard optics. Left curve shows the intensity distribution along the vertical axis. KrF and XeCl produce broader, more flat-topped distributions. Right curve shows the horizontal intensity distribution. Data were obtained using a Laser Probe detector array from Spincon, Inc., Logan, Utah.

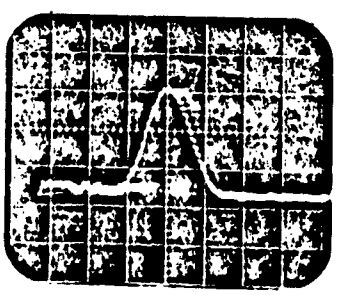

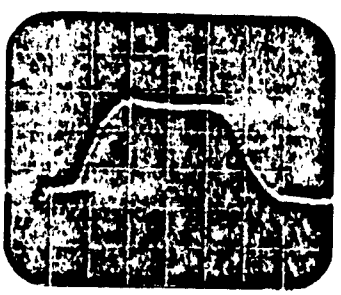

Timing sequence for a laser at turn-on. Trace was obtained using a photodiode detector, and the "spike" corresponds to the laser pulse.

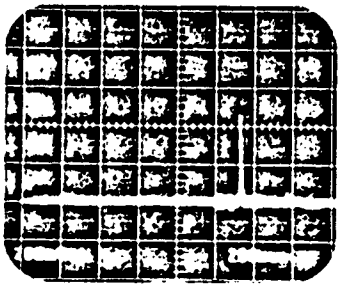

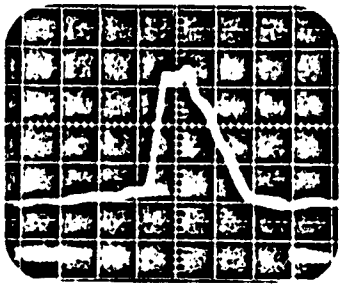

Superposition of multiple laser pulses for KrF. Note the excellent pulse amplitude stability as well as low jitter.

Jitter

Timing jitter is defined as changes in the time interval between an external trigger and the laser pulse. Long-term timing jitter (minutes or hours) is usually called "drift" and is quite different from short-term jitter (a few pulses). However, both are usually caused by the same effect—a change in voltage translated to a change in time by the finite frequency response of the system.

The oscillogram shows the timing sequence for a laser at turn-on. The laser pulse is delayed from an external trigger by approximately 1100ns. Noise from the thyratron firing begins at 1000ns and the laser pulse follows approximately 150 ns later.

Long-term jitter

Long-term jitter, or drift in the delay time is caused by thermal effects in the thyratron. As the thyratron temperature reaches equilibrium after turn-on, the switching time decreases (as shown in the graph below) then remains constant to approximately ± 2ns for long periods of time. Any change in thyratron loading, caused by variations in high voltage, reservoir voltage or repetition rate, will cause this time to change.

Short-term jitter

Short-term jitter also depends on the high voltage regulation because both the thyratron switching and gas discharge in the cavity are voltage-dependent and change at the rate of several ns/kV. In addition, the choice of thyratron is important; a conventional grounded-cathode thyratron in the "glow" mode has less inherent jitter than a grounded grid thyratron and is less sensitive to tube loading. The oscillogram on the upper right is a time exposure of 1000 pulses at 100Hz and shows timing jitter less than ± 2ns.

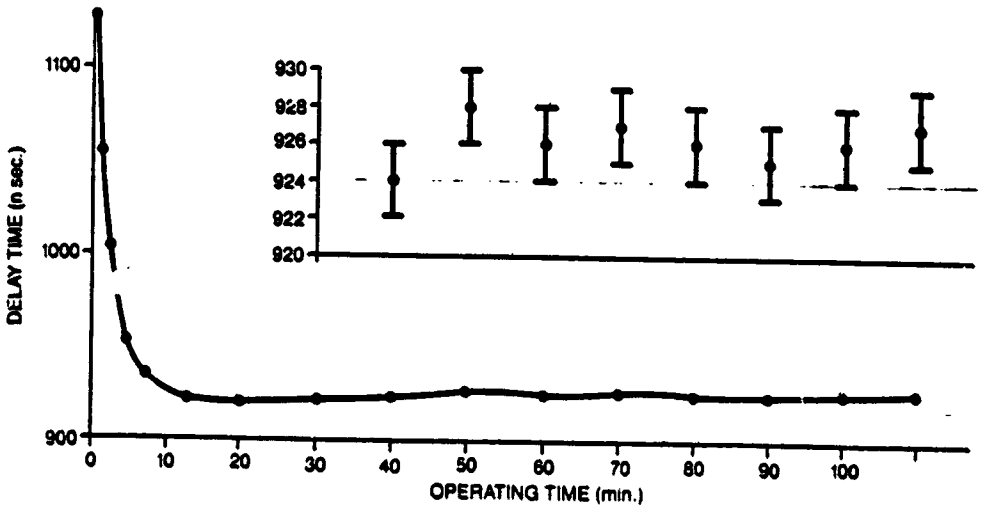

Delay time from external trigger to laser pulse as a function of operating time. Data at extended operating times are shown on an expanded scale in the inset for clarity. Vertical bars on data points represent uncertainty of the measurements.

Optional Accessories

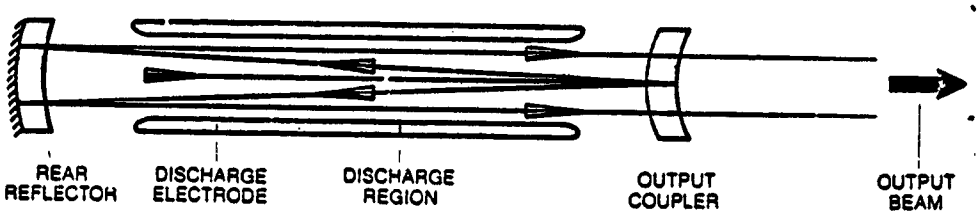

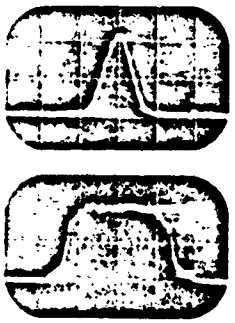

Scanned array beam profiles for ArF with unstable resonator optics. Note the smooth intensity distributions and the absence of "holes."

Unstable Resonator Optics

Low-divergence operation of excimer lasers is important for applications which require either high-collimation for beam transport, enhanced focussing for high resolution, or increased brightness for non-linear processes. Standard, stable resonator configurations for all excimer lasers produce output beams with divergences of several milliradians. Questek designed the Model 2030 Unstable Resonator Optics to provide efficient and economic low-divergence operation.

Positive-branch, unstable resonator configurations have always offered a means to reduce divergence, but typically at great expense of output energy in the far-field. In addition, unstable resonator optical designs often result in a "hole" in the intensity distribution which diffracts away only very slowly so that uniform intensity distributions are difficult to realize in practice.

The optical configuration of the Model 2030 cavity results in high operating efficiencies: at least 85% of the specified stable resonator energy in the near-field for KrF and XeCl and 65% in near-field for ArF. Fully ¾ of the near-field energy is available in far-field with beam divergences reduced to 200–400 microradians. Such optical efficiencies are a factor of two higher than other lasers with unstable resonator optics, and the divergence is comparable to more complex injection-locked systems.

Because high reflectivity 'dot' coatings are not used on the output coupler, the beam intensity distribution is smooth, flat-topped and without "holes"—as shown by the scanned-array profile. The model 2030 was designed for intracavity use without intervening 'offset' windows, resulting in greater extraction efficiency. This simple design means that the Model 2030 is a direct replacement for standard, stable resonator optics so installation and alignment are fast and straightforward. The unstable resonator optics normally come with broadband coatings for operation at different wavelengths; single-wavelength, dielectric-coated optics are also available on request.

He-Ne Beam Aligner

In many applications it is important to know the precise direction of the excimer laser beam without actually running the laser. The optional Model 2070 He-Ne Beam Aligner mounts behind the rear mirror of the cavity—the He-Ne beam travels through the dielectric coating on the rear mirror, down the cavity axis, and out the front mirror on the laser axis. Although intended primarily to be a beam pointer, the He-Ne laser can also be used to align the cavity optics.

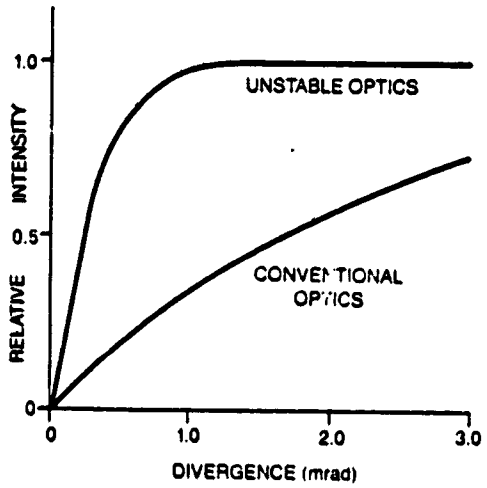

Normalized beam intensities as a function of divergence angle for conventional and unstable configurations.

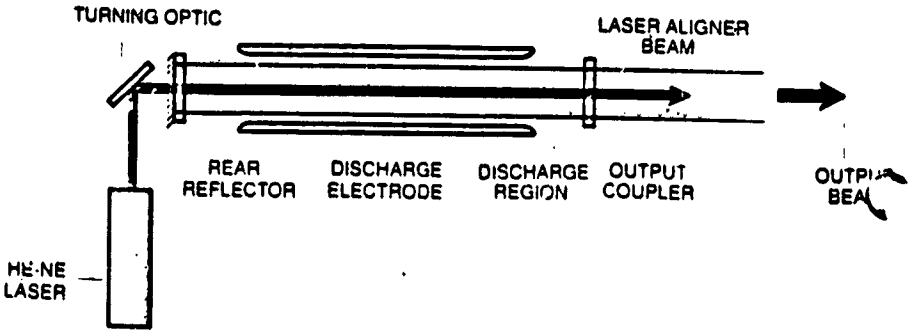

Cryogenic gas processing

Both particulate and gaseous contaminants shorten gas lifetimes. While particulates can be removed by a mechanical filter, gaseous contaminants must be removed by cryogenic trapping or chemical processing. Given the simplicity of cryogenic processing, this technique provides the most cost-effective means for removing gaseous contaminants, and it is the one used in most excimer lasers.

The impact of gaseous contaminants on laser output increases at shorter wavelengths; for XeCl the particulates are more important, for KrF both particulate and gaseous contaminants are important, while for ArF the gaseous contaminants are the dominant cause of short lifetime. However, in all cases the particulates must be removed and the optics "washed" with clean gas to keep them clean.

The adjacent figure shows the vapor pressure of various excimer gases and typical contaminants as a function of temperature. Each excimer mixture requires a different temperature to maximize contaminant trapping without "freezing out" the excimer gases. ArF operates at the lowest temperature, near that of liquid nitrogen (77 degrees Kelvin) while the other gas mixtures require temperatures up to about 135 degrees Kelvin.

Questek offers as an option in the U.S. and Canada the GP2000 temperature-controlled cryogenic gas processor manufactured by Oxford Lasers Ltd. This system is designed specifically for excimer lasers and covers the required temperature range using liquid nitrogen as the coolant. A pump-out port is provided to remove trapped contaminants when the system warms up.

All Series 2000 lasers are supplied with standard bulkhead fittings on the rear utilities panel to simplify connection to an external gas processor. When a cryogenic processor is used, the standard Questek processor is removed, and the cryogenic system is attached as shown in the figure.

In general, cryogenic gas processing will extend the useful gas lifetime of ArF and KrF by a factor of 5 to 10, depending on operating conditions. Given the short lifetime of ArF without cryogenic processing and the high cost of KrF, the added lifetime achieved through cryogenic processing is a major benefit for these gases.

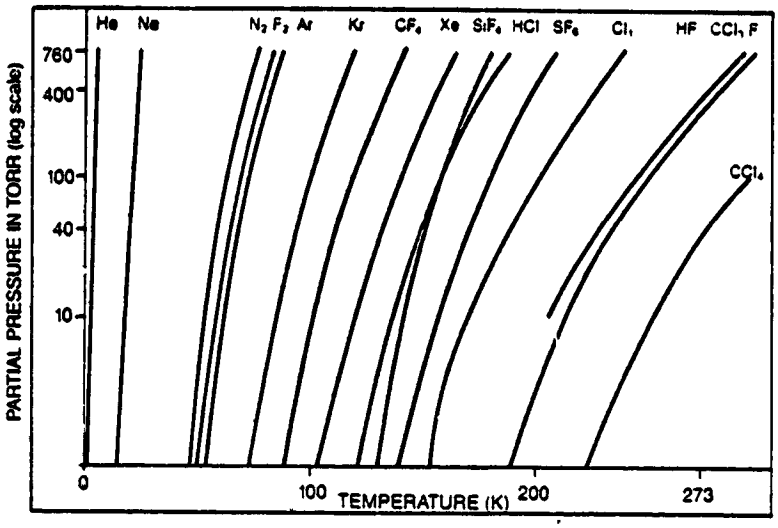

*Vapor pressure of various excimer gases (shown in black) and typical contaminants as a function of temperature. Shaded region shows the operating range of the GP2000.**

**GP2000 is a trademark of Oxford Lasers Ltd.*

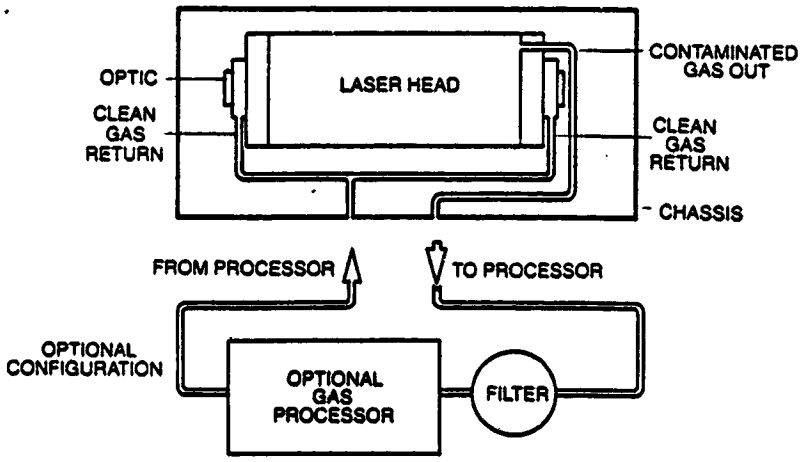

Cyrogenic gas processor configuration, showing particulate filter, GP2000 gas purifier, and circulation loop.

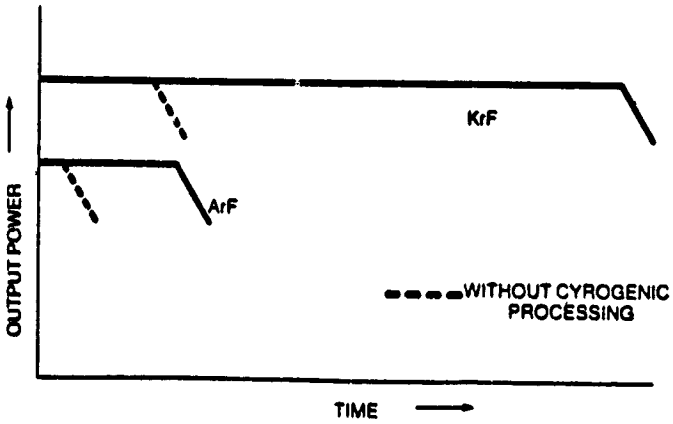

Laser output power as a function of time for ArF and KrF using cryogenic gas processing. Results are typical but depend in detail on particular operating conditions.

Choosing the Model

The Series 2000 family of excimer lasers spans a wide range of performance parameters with models which offer maximum single-pulse energies of ¾ J or lower pulse energy operation with repetition rates to 400 Hz. The entire family is divided into four groups of models designated as Models 22xx, 24xx, 26xx, and 28xx, according to the magnitude of the stored energy and the configuration of the electrode assembly. These groups are further divided into sub-categories according to average power capacity and designated by model numbers xx20, xx40 or xx60. For example, the Model 2260 is the highest repetition rate version of the lowest pulse energy models. In addition, each model can operate with reduced pulse energy at twice the normal repetition rate.

Each model is interchangeable with any other; that is, any model can be converted in the field to any other. To change energy but not average power, the primary capacitors and electrode assembly are replaced. To increase average power but not pulse energy, the power supply and thyratron are changed. To increase the maximum repetition rate at a sacrifice in energy, the primary capacitors are changed. In choosing a model for a particular application it is important to keep in mind that operation at reduced pulse energies is required for long-term performance under Powerlok. Calculate the pulse energy required and equate this to 60–75% of the specified output.

High energy lasers have significantly shorter gas lifetimes than lower energy lasers because more energy is delivered to the gas during each pulse. The relationship is not linear—a laser with twice the energy may have one-fourth the gas lifetime (measured in pulses) of a smaller laser.

Immediately upon receipt of an order, Questek's customer support group will send a site-preparation letter containing all of the information required to set up and install the laser. Following delivery, a Questek engineer will test the laser on site with one gas mixture and train one or more users in operation and maintenance of the laser. These services are standard and included in the price of the laser.

Commitment to Customer Support

Questek realizes that customer support in the field is an essential ingredient to building a sound business. Our commitment to service is demonstrated by the fact that our interaction with a user is just beginning, not ending, when we deliver a laser. Following installation we maintain contact with quarterly newsletters describing new features and operating modes and relaying information received from our users. When travelling in the area, our staff will visit a user to see how the laser is performing. We value the rapport we establish, and the knowledge we receive from our users helps us to improve our products and our business.

Questek also operates a well-equipped applications laboratory for use by visitors on a fee basis. First-time users pay a reduced fee and a portion of all payments are applied toward the purchase of a laser.

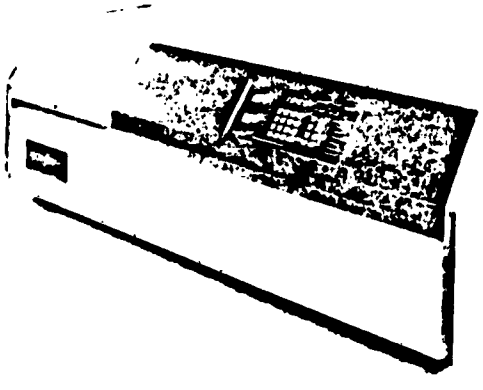

Series 2000 Excimer Laser Specifications

	ArF	KrF	XeCl	XeF	Units
Wavelength	193	248	308	351	nm
2200 Models					
Pulse energy	200	300	200	150	mJ
Average power					
Model 2220 (50Hz)	8	12	8	6	W
Model 2240 (100Hz)	15	24	16	12	W
Model 2260 (200Hz)	24	45	30	22	W
2400 Models					
Pulse energy	275	400	275	200	mJ
Average power					
Model 2420 (40Hz)	8	12	8	6	W
Model 2440 (80Hz)	15	24	16	12	W
Model 2460 (150Hz)	24	45	30	22	W
2600 Models					
Pulse energy	350	600	350	300	mJ
Average power					
Model 2620 (25Hz)	7	12	7	5	W
Model 2640 (50Hz)	13	24	14	10	W
Model 2660 (100Hz)	21	40	25	20	W
2800 Models					
Pulse energy	400	750	400	350	mJ
Average power					
Model 2820 (20Hz)	6	12	6	5	W
Model 2840 (40Hz)	11	24	12	10	W
Model 2860 (80Hz)	20	40	22	20	W
Pulse-to-pulse stability[1]	±6	±5	±3	±5	%
Pulse duration (nominal FWHM)[2]	10–25				ns
Beam dimensions (V × H)	8–13 × 20				mm
Beam divergence (V × H)	2 × 3				mr
Timing jitter from external trigger[1]	±2				ns

[1] 90% of pulses.

[2] Depends on gas mixture and pulse energy.

Note: All models can operate with reduced energy at twice the normal repetition rate. Consult the factory for details

All specifications subject to change without notice.

Weight:
Laser: 560 lbs. (255 Kg)
Pump: 42 lbs. (19 Kg)
Shipping: 720 lbs. (327 Kg)

Power Required
220V, 50/60Hz, single phase
Models xx20: 20A
Models xx40: 25A
Models xx60: 30A

Cooling Water:
Models xx20: 0.5 GPM
Models xx40: 1.0 GPM
Models xx60: 1.5 GPM

INVISIBLE LASER RADIATION—
AVOID EYE OR SKIN EXPOSURE
TO DIRECT OR SCATTERED
RADIATION

Maximum average power: 100W
Maximum pulse energy: 3J
Pulse duration: 10–1000ns
Wavelength: 157–351 nm
10.6 μm

CLASS IV LASER PRODUCT

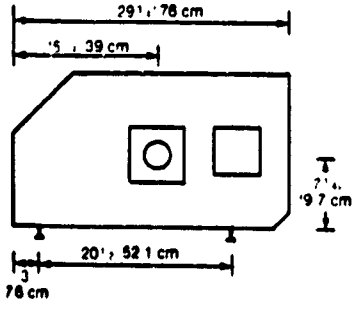

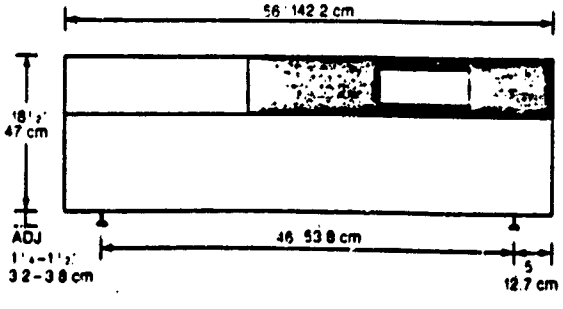

Background

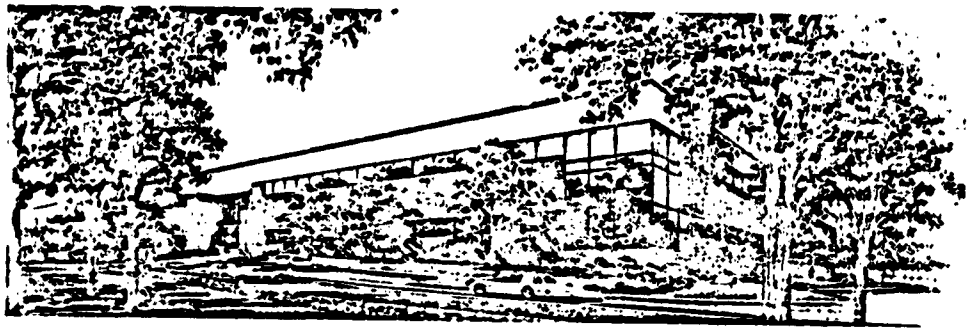

Questek Firsts

- Microprocessor laser control
- Powerlok constant power control
- Automatic gas filling & replenishment
- Built-in energy power monitor
- Elimination of reverse aftercurrent
- Unlimited electrode lifetime
- High efficiency design emphasizing reliability
- Remote diagnostics
- Toll-free customer support number

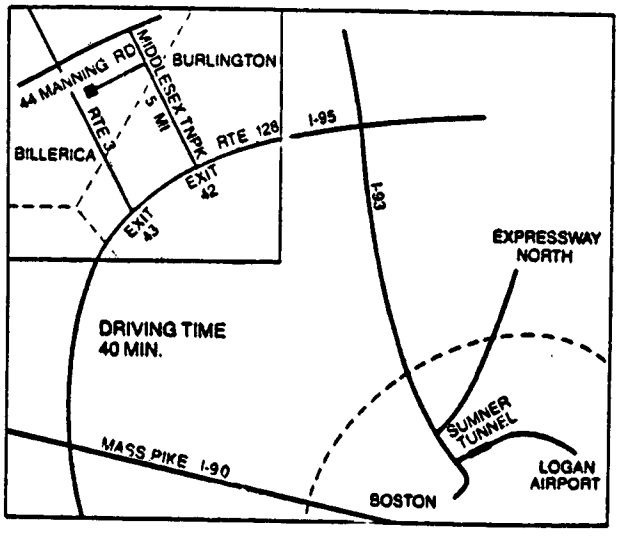

Questek was formed in October, 1982, to manufacture excimer lasers which fulfilled not only the high performance requirements of the existing scientific R & D market, but also the stringent need for reliability and ease of operation required by industrial and medical applications. The three founders of the Company brought with them more than 30 years of collective experience in commercial pulsed laser technology. They shared a commitment for excellence and had an established reputation in the industry for providing strong customer support.

In Spring, 1983 Questek introduced its first product line, the Series 2000 Excimer Lasers. The Series 2000 incorporated many new features never before available in commercial excimer lasers, including Powerlok,™ a microprocessor-based control system to provide constant laser output power. The uniqueness of the Series 2000 signalled nothing less than the arrival of a new generation of excimer lasers, as confirmed by the subsequent efforts of other manufacturers to duplicate the features and performance available with these lasers.

In 1984, the first year of product shipments, Questek delivered more than forty lasers and established itself as the largest U.S. manufacturer of excimer lasers. In the second year of shipments the company more than doubled in size and moved to the new facilities shown.

The strong acceptance of the Series 2000 Excimer Lasers in the scientific market and in industrial and medical laboratories has made Questek one of the fastest growing laser manufacturers in the history of the industry. The rapidly increasing customer base is an affirmation of Questek's commitment to provide quality products with innovative features coupled with strong technical support and personalized customer service.

QUESTEK

QUESTEK INC.
44 Manning Road
Billerica, MA 01821

Tlx: 4971358 Questek

Tel: 617-667-6790
1-800 EXCIMER (U.S. only)

Printed in USA 4 85 10M

© QUESTEK INC. 1985

Appendix B

SAMICS INPUT

Data for Samics input for pulsed excimer laser annealing was calculated from enclosed estimates furnished by Questek. All monetary values are in 1985 dollars.

One 50 watt laser is assumed to be scanning the surface of wafers as they are being moved from a cassette (unloader) to the front contact screen printer. Possible changes to the required transport system are minimal and neglected here. The optical scanning system is assumed to consist of a set of X-Y rotating mirrors, a linear translator for dynamic focus, and driver electronics from General Scanning Inc. (Watertown, MA 02272). One UV focussing lens is required.

Manufacturers' quotes were used to estimate capital equipment cost, which includes essential spart parts. Electricity and air conditioning load for the system was estimated at 5kW. The use of gas and spare parts is directly from the Questek quote, computed per minute. Power and parts for the scanner were estimated.

The laser requires periodic venting to the atmosphere (every 2 hours) of approximately 3 cubic feet of krypton, helium and a much smaller amount of flourine. The cost of these byproducts was not included. Downtime for gas changes was included.

SOLAR ARRAY MANUFACTURING INDUSTRY COSTING STANDARDS
FORMAT A - PROCESS DESCRIPTION

JET PROPULSION LABORATORY
California Institute of Technology
4800 Oak Grove Dr., Pasadena, CA 91109

☐ A-1 Process [Referent]
P E L A
Revision Number: 1

Note: Names given in brackets [ ] are the names of process attributes requested by the SAMIS Computer Program.

☐ A-2 [Descriptive . Name] of process PULSED EXCIMER LASER ANNEAL (OF ION IMPLANTED N+P JUNCTIONS)

PART 1 - PRODUCT DESCRIPTION

☐☐ A-3 [Product . Referent] ANNEALED SLICE
A-5 Unit of Measure [Product . Units] M^2

☐ A-4 Descriptive Name [Product . Name] WAFER (SLICE) WITH N+P JUNCTION

PART 2 - PROCESS CHARACTERISTICS

☐ A-6 [Output . Rate] (Not Thruput) 0.1 M^2/min — Units (given on line A-5) Per Operating Minute

☐ A-7 [Inprocess . Inventory . Time] .083 — Calendar Minutes

☐ A-8 [Duty . Cycle] .80 — Operating Minutes Per Minute

☐ A-8a [Number . Of . Shifts . Per . Day] 3 — Shifts

☐ A-8b [Personnel . Integerization . Override . Switch] ____ (Off or On)

PART 3 - EQUIPMENT COST FACTORS [Machine . Description]

☐ A-9 Component [Referent]	LASER	SCANNER	
☐ A-9a Component [Descriptive . Name]	KrF Excimer Laser 50 watts (Questek)	Scanning Mirror Assembly	
☐ A-10 Base Year for Equipment Prices [Price . Year]	1985	1985	
☐ A-11 [Purchase . Cost . Vs . Quantity . Bought . Table] (Number Of and $ Per Component)	1 65.6K	1 8.3K	
☐ A-12 Anticipated [Useful . Life] (Years)	5	5	
☐ A-13 [Salvage . Value] ($ Per Component)	5K	2K	
☐ A-14 [Removal . And . Installation . Cost] ($/Component)	5K	1K	
[Payment . Float . Interval]	0.0	0.0	0.0
[Inflation . Rate . Table]	IRTJ	IRTJ	IRTJ
[Equipment . Tax . Depreciation . Method]	DDB	DDB	DDB
[Equipment . Book . Depreciation . Method]	SL	SL	SL

K = $1000

A-15 Process Referent (From Front Side Line A-1)

PART 5a - BYPRODUCTS PRODUCED PER MACHINE PER MINUTE [Byproduct]

A-20 Catalog Number (Expense Item Referent)	A-22 Amount Produced Per Machine Per Minute [Amount . Per . Cycle]	A-23 Units	A-21 Byproduct Specifications

PART 4 - FLOORSPACE PER MACHINE and PERSONNEL PER MACHINE PER SHIFT [Facility . Or . Personnel Requirement]

A-16 Catalog Number (Expense Item Referent)	A-18 Amount Required [Amount . Per . Machine]	A-19 Units	A-17 Requirement Description
A 2 0 6 4 D	32	Sq. Ft.	Mgf space type A
B 3 0 9 6 D	0.5	Prs. * Yrs	Operator (Semiconductor Assembler)
B 3 7 0 4 D	0.1	Prs. * Yrs	Maintenance (Electronic Technician)

PART 5b - DIRECT REQUIREMENTS PER MACHINE PER MINUTE [Utility . Or . Commodity Requirement]

A-20 Catalog Number (Expense Item Referent)	A-22 Amount Required Per Machine Per Minute [Amount . Per . Cycle]	A-23 Units	A-21 Requirement Specifications
C 1 0 3 2 B	.0417	kw.Hr./min	Electricity
C 2 0 9 6 B	.0417	kw.Hr./min	Air Conditioning
	.0057	Dollars/min.	Fluorine Gas
	.1333	Dollars/min.	Krypton Gas
	.0167	Dollars/min.	Helium Gas
E 1 6 0 8 D	.1655	Dollars/min.	Spare parts
	.0077	Dollars/min	Liquid Nitrogen

PART 6 - INTRA-INDUSTRY PRODUCT(S) REQUIRED

A-24 [Required . Product] (Reference)	A-28 [Yield] (%)	A-26 [Ideal . Ratio] Of Units Out/Units In	A-27 Units of A-26	A-25 Product Name

PREPARED BY	COMPANY	DATE	JPL USE ONLY
CHECKED BY	COMPANY	DATE	